

**Vibrations of small cobalt clusters on low-index surfaces of copper: Tight-binding simulations**S. D. Borisova,<sup>1</sup> S. V. Ereameev,<sup>1</sup> G. G. Rusina,<sup>1</sup> V. S. Stepanyuk,<sup>2</sup> P. Bruno,<sup>2,3</sup> and E. V. Chulkov<sup>4,5,\*</sup><sup>1</sup>*Institute of Strength Physics and Materials Science, pr. Akademicheskii 2/1, 634021, Tomsk, Russia*<sup>2</sup>*Max-Planck-Institut für Mikrostrukturphysik, Weinberg 2, 06120 Halle, Germany*<sup>3</sup>*European Synchrotron Radiation Facility, BP 220, F38043 Grenoble Cedex, France*<sup>4</sup>*Donostia International Physics Center (DIPC), Paseo de Manuel Lardizabal 4, 20018 San Sebastián/Donostia, Basque Country, Spain*<sup>5</sup>*Departamento de Física de Materiales and Centro Mixto CSIC-UPV/EHU, Facultad de Ciencias Químicas, Universidad del País Vasco/Euskal Herriko Unibertsitatea, Apartado 1072, 20080 San Sebastián/Donostia, Basque Country, Spain*

(Received 2 April 2008; revised manuscript received 24 June 2008; published 20 August 2008)

Vibrational properties (frequencies, polarizations, and lifetimes) of a single adatom, dimer, and trimer of Co on low-index Cu surfaces, Cu(111), Cu(001), and Cu(110) are studied by using tight-binding second moment approximation interatomic interaction potentials. We show that structural and vibrational properties of the Co clusters strongly depend on the substrate orientation. The longest lifetimes of 1–2.5 ps have been found for high-frequency *z*-polarized vibrations in all the Co clusters considered. The shortest lifetimes of 0.1–0.8 ps have been obtained for low-frequency horizontal (frustrated translation) vibrational modes.

DOI: [10.1103/PhysRevB.78.075428](https://doi.org/10.1103/PhysRevB.78.075428)

PACS number(s): 63.20.D-, 63.22.-m, 68.35.Ja, 68.43.Hn

**I. INTRODUCTION**

Phonons on clean metal surfaces and surfaces covered with overlayers have widely been investigated for the last decades both experimentally<sup>1–5</sup> and theoretically.<sup>4,6–10</sup> Experimentally vibrational modes on surfaces are normally measured by helium atom scattering (HAS) (Ref. 11) technique or by electron energy-loss spectroscopy (EELS).<sup>12</sup> However, recently surface phonons have been measured locally with atomic resolution by inelastic electron-tunneling spectroscopy (IETS).<sup>13</sup> In general, characteristic vibrational features on surfaces and in overlayers such as gap phonons on alkali and other metal surfaces,<sup>4,8,11,12,14–19</sup> surface resonance vibrations,<sup>2,20,21</sup> step vibrational modes on vicinal surfaces,<sup>6,7,22,23</sup> overlayer phonon states,<sup>3,9,24</sup> adatom-substrate stretch vibrations and the frustrated translation mode frequencies in submonolayer coverages<sup>3,9,10,25–27</sup> are rather well understood. In these systems, vibrational modes are delocalized over an entire area (surface, lateral overlayer area, step-one dimensional area).

Despite important role that vibrational properties of small clusters (including a single adatom) play in understanding of many phenomena such as surface reactions, desorption, adsorbate diffusion, island and film growth, lubrication, and friction<sup>28</sup> significantly less is known about vibrations of metal clusters on metal substrates. This can be accounted for by two reasons. Experimental study of small cluster vibrations requires the use of local technique such as IETS.<sup>13,29</sup> However, until now, the IETS measurements have been done only for some molecules on metals (for references see, for instance Ref. 13). Theoretical study requires *ab initio* calculations or evaluations based on accurate interatomic interaction potentials and very big unit cells. The latter factor makes *ab initio* calculations very time consuming. In the present work we study vibrational properties (frequencies, polarizations, and lifetimes) of small Co clusters (dimer and trimer) on low-index Cu surfaces by using many-body interatomic potentials developed by Levanov *et al.*<sup>30</sup> and Stepanyuk *et al.*<sup>31</sup> within tight-binding second moment approximation

(TB-SMA). We also present the calculation results for a single Co atom on the Cu surfaces.

The Co/Cu system has been chosen as an important model system since such phenomena as diffusion, growth, and structure were extensively investigated both experimentally and theoretically. Kief and Egelhoff<sup>32</sup> have reported the observation of Co film growth on low-index Cu surfaces, characterized by the formation of compact Co clusters. Using DFT calculations, Pentcheva *et al.* analyzed possible equilibrium structures for a monolayer coverage of Co on Cu(001).<sup>33</sup> They found that a flat Co film on the top of the Cu(001) surface should be a stable structure, whereas the preferred structure was found to be a bilayer Co island covered by a Cu monolayer. However, since island growth is a nonequilibrium process, the surface crystal structure is determined by the kinetic processes. The Co/Cu surface exchange can result in a variety of structures, such as a Co/Cu surface alloy,<sup>34</sup> Cu-covered Co islands,<sup>32</sup> and Co-covered Cu islands.<sup>33,35</sup>

TB-SMA simulations for Co islands and steps on Cu(111) revealed that adsorbate-induced strain in the substrate makes surface diffusion of Co adatom anisotropic: the migration barrier exhibits strong oscillations near the island edges.<sup>36</sup> By using accelerated molecular dynamics<sup>37</sup> and TB potentials<sup>30</sup> it was found that upward-transport mechanism at island edges is responsible for the bilayer Co island formation at low temperatures. At high temperatures diffusion of Co into the surface produces qualitative changes in the island structure, leading to the reversal of the low-temperature transport mechanisms and resulting in a monolayer growth. It was found that small Co clusters (dimers, trimers, and heptamers) significantly affect the low-coverage morphology due to high translational and rotational mobility of the clusters.<sup>38</sup>

The dynamics of a single Co adatom during lateral manipulation on a copper (111) surface by a low-temperature scanning tunneling microscope was investigated by Stroschio and Celotta<sup>39</sup> and later on was studied by Liu and Gao.<sup>40</sup> It was shown that the frustrated translation (FT) mode is responsible for the lateral hopping. The calculated frequency

shows good agreement with the onset energy for the adatom hopping induced by inelastic tunneling. The detailed study of the FT mode of a single Co adatom on Cu(111) has been carried out in Ref. 41.

Here we give a detailed analysis of horizontal (FT) and vertical vibrational modes, including lifetimes, for small Co adclusters on Cu(111), Cu(110), and Cu(001). We show that frequencies of these modes, their intensities, and coupling with the substrate atoms strongly depends on the Cu substrate orientation.

The paper is organized as follows. In Sec. II we give a short description of the computational method used. In Sec. III, first, we analyze in details the equilibrium atomic structure of the Cu surfaces with the Co adclusters and the Co–Cu bonding on the Cu substrates since it plays a key role in vibrations of the adsorbed clusters. Then the comparative analysis of vibrations of a single Co adatom, dimer, and trimer on low-index Cu surfaces is carried out. Finally, conclusions are given in Sec. IV.

## II. COMPUTATIONAL METHOD

The present calculations of crystal structure and vibrations of small Co clusters on the low-index Cu surfaces are based on interatomic interaction potentials Cu–Cu, Cu–Co, and Co–Co obtained in the second moment tight-binding approximation.<sup>42</sup> In this approximation the total energy of a system is given as a sum of band energy (electronic cohesive energy or the attractive term),  $E_B$ , and a repulsive energy,  $E_R$ , of the constituent atoms

$$U_{\text{tot}} = \sum_i U_i = \sum_i (E_B^i + E_R^i), \quad (1)$$

Here summation is carried out over all positions of atoms of a system. The band energy term represents many-body interatomic interactions

$$E_B^i = - \left\{ \sum_{j \neq i} \xi_{\alpha\beta}^2 \exp[-2q_{\alpha\beta}(r_{ij}/r_0^{\alpha\beta} - 1)] \right\}^{1/2}, \quad (2)$$

the repulsive term is described by a pair modified Born-Mayer repulsive potential

$$E_R^i = \sum_{j \neq i} \phi_{ij}(r_{ij}), \quad (3)$$

$$\phi_{ij}(r_{ij}) = (A_{\alpha\beta}^1 (r_{ij}/r_0^{\alpha\beta} - 1) + A_{\alpha\beta}^0) \exp[-p_{\alpha\beta}(r_{ij}/r_0^{\alpha\beta} - 1)]. \quad (4)$$

In Eqs. (2)–(4)  $r_{ij}$  is the distance between atoms  $i$  and  $j$ ,  $\alpha$  and  $\beta$  denote different atomic species,  $r_0^{\alpha\beta}$  is the first neighbor distance in bulk pure metals ( $\alpha = \beta$ ) and is an adjustable parameter for the  $\alpha \neq \beta$  case,  $\xi_{\alpha\beta}$  is an effective hopping integral for the first neighbor atoms. Parameters  $q_{\alpha\beta}$  and  $p_{\alpha\beta}$  describe the decay of the interatomic interaction strength. The parameters for the Cu–Cu interaction had been fitted to experimental data for bulk Cu only.<sup>42</sup> The Cu–Co and Co–Co potentials were fitted to KKR density functional in the local spin-density approximation calculation results obtained for binding energy of small supported Co clusters on Cu(001) and two Co impurities in bulk Cu.<sup>30,43</sup>

Previous studies<sup>37,44–46</sup> have demonstrated that the combination of *ab initio* and the tight-binding methods allows one to construct many-body potentials which provide reliable description of interatomic interactions, and atomic relaxations in low-dimensional systems. Very recent experimental work has confirmed the scenario of atomic relaxations in Co clusters on Cu(001) predicted by our approach.<sup>47,48</sup>

To determine the equilibrium atomic structure, we relax the surfaces with adsorbates using standard molecular-dynamic technique based on the TB interaction potentials described above. To simulate a semi-infinite Cu metal with a single adatom, dimer, and trimer of Co on the metal surface a thin-film model of a two-dimensional periodic slab consisting of 31 atomic layers of Cu(111) or Cu(001) with supercells  $(3 \times 3)$ ,  $(4 \times 4)$ , and  $(5 \times 5)$  to exclude direct interactions adatom–adatom, dimer–dimer, and trimer–trimer is used. For Cu(110) we use  $(3 \times 4)$ ,  $(3 \times 5)$ , and  $(3 \times 6)$  supercells. For large supercells the calculations have also been carried out for 25 layer film thickness. The chosen thicknesses prevent interactions between two opposite surfaces of the film. The calculations of vibrational spectra are carried out by the dynamical matrix method. Diagonalizing the matrix gives the eigenfrequencies and the polarization vectors of vibrations. The local vibration densities of states were obtained by projecting these eigenmodes onto atoms of interest in a given ( $x+y$  or  $z$ ) direction. The lifetimes of vibrational modes are calculated by fitting the peaks of the local density of vibrational states by a Lorentzian function.

## III. CALCULATION RESULTS AND DISCUSSION

### A. Atomic structure

First, we briefly discuss atomic structure of unsupported (free standing) small Co clusters (dimer and trimer) and clean low-index Cu surfaces (111), (001), and (110). The calculated equilibrium bond length (distance between Co atoms) of the free dimer is found to be of 2.23 Å. This result is in agreement with the experimental dimer bond length of 2.31 Å (Ref. 49) and slightly differs from the density-functional theory (DFT) calculation values of 1.92–1.96 Å (Refs. 50 and 51) as well as from a tight-binding Hubbard Hamiltonian (TBHH) calculation result of 2.47 Å.<sup>52</sup> The evaluated binding energy of the dimer, 1.43 eV/atom, agrees well with that of 1.45 eV/atom obtained from the DFT calculation.<sup>50</sup> Both these values are in between experimental data of 1.73 (Ref. 49) and 1.32 eV.<sup>53</sup> The latter energy is the upper limit for the dimer dissociation energy derived from collision-induced dissociation experiments.<sup>53</sup>

The most stable form of the free Co trimer obtained from our calculation is an equilateral triangle with the bond length of 2.33 Å which is slightly longer than the calculated dimer bond length. The calculated free chain of three Co atoms has bond length of 2.27 Å which is shorter than that in the triangle cluster but slightly longer than the dimer bond length. The calculation shows that the chain lies 0.30 eV/atom higher than the equilibrium triangle. As in the case of the Co dimer our bond length is slightly longer than that obtained from DFT calculations [2.06–2.25 Å (Refs. 50 and 51)] and shorter compared to the TBHH result [2.55 and 2.69 Å (Ref.

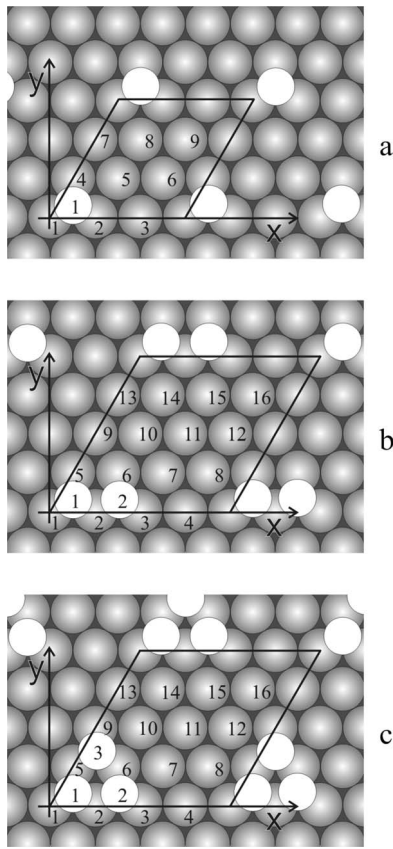


FIG. 1. Adsorption structures for (a) a single Co adatom,  $p(3 \times 3)$ , (b) a dimer,  $p(4 \times 4)$ , and (c) a trimer,  $(4 \times 4)$  on the Cu(111) surface. The calculation supercells are indicated by a rhombus. Here  $x=[1\bar{1}0]$  and  $y=[11\bar{2}]$ .

52)]. The calculated binding energy of 1.89 eV/atom is in fairly good agreement with the DFT calculation by Datta *et al.*,<sup>50</sup> 1.78 eV/atom, and with *ab initio* calculation by Castro *et al.*,<sup>51</sup> 1.53–3.67 eV/atom. The equilateral triangle configuration of the Co cluster agrees with both *ab initio* and TBHH calculation results for  $\text{Fe}_3$  and  $\text{Ni}_3$  clusters which also form an equilateral triangle.<sup>51,52</sup> However, these calculations give an isosceles triangle as ground state for the  $\text{Co}_3$  cluster with small difference in the sides length. Castro *et al.*<sup>51</sup> obtained a triangle whose two equal sides are shorter than the third side; while in the calculation by Datta *et al.*<sup>50</sup> two equal sides are longer than the third one. These distinct results can be accounted for by a very small difference in total energy between different cluster geometries. For instance, our total-energy calculation gives an isosceles triangle with small difference in the sides length whose energy is only few meV/atom higher than the equilateral triangle energy. This little inaccuracy of the Co-Co potentials does not affect the Co cluster structure and vibrations on Cu surfaces since the cluster geometry on the substrate is strongly affected by the Cu-Co interactions (see Figs. 1–3). As we show below (subsection B, Vibrations) the most important consequence for the free standing  $\text{Co}_3$  concerning the distinction of the isosceles triangle from the equilateral one is the slight splitting of the lower vibrational mode in two ones.

The evaluated equilibrium atomic structure of the clean Cu(111), Cu(001), and Cu(110) surfaces slightly differs from

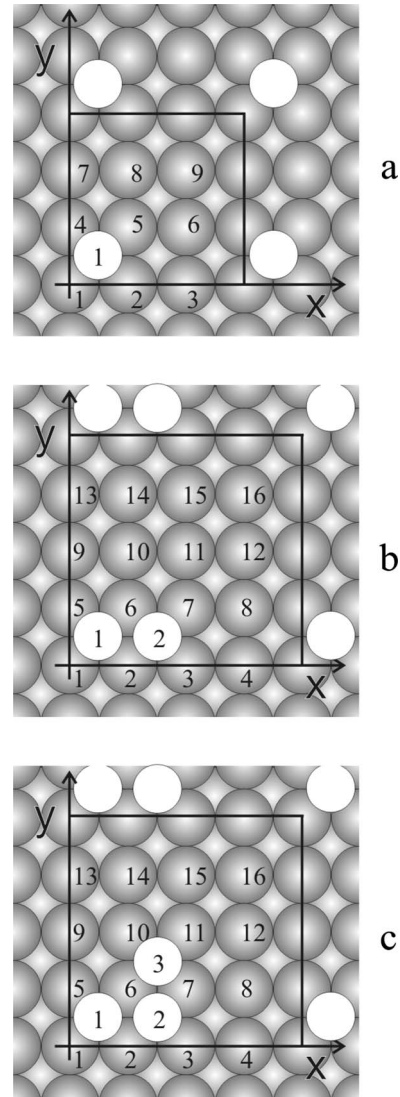


FIG. 2. Adsorption structures for (a) a single Co adatom,  $p(3 \times 3)$ , (b) a dimer,  $p(4 \times 4)$ , and (c) a trimer,  $(4 \times 4)$  on the Cu(001) surface. The calculation supercells are indicated by a square ( $x=[110]$  and  $y=[\bar{1}10]$ ).

the ideal one by small alterations of the first and second interlayer spacings. On Cu(111), both interlayer spacings are contracted (inward relaxation) with the relative values  $\Delta_{12} = -0.90\%$  and  $\Delta_{23} = -0.14\%$  which are in excellent agreement with available experimental and theoretical data. The relative contractions of the interlayer distances measured by using medium-energy ion scattering are  $\Delta_{12} = -1.0\% \pm 0.4\%$  and  $\Delta_{23} = -0.2\% \pm 0.4\%$ .<sup>54</sup> The value of the first interlayer contraction obtained from first-principles calculations<sup>55</sup> is  $-0.9\%$ . On Cu(001), the obtained interlayer spacings are also contracted and, compared to the bulk interlayer spacing, they are:  $\Delta_{12} = -1.20\%$  and  $\Delta_{23} = -0.37\%$ . On this surface, even the third interlayer spacing is slightly contracted,  $\Delta_{34} = -0.05\%$ . These values are well compared to embedded atom model calculation results:  $\Delta_{12}$  is  $-1.21\%$  (Ref. 56) and  $-1.44\%$ ,<sup>57</sup>  $\Delta_{23} = -0.33\%$ .<sup>57</sup> The obtained  $\Delta_{12}$  is also in fairly good agreement with experimental results,  $\Delta_{12} = -1.1\%$  (low-energy electron-diffraction (LEED)),<sup>58</sup>  $\Delta_{12} = -1.1\%$  (MEIS),<sup>59</sup>

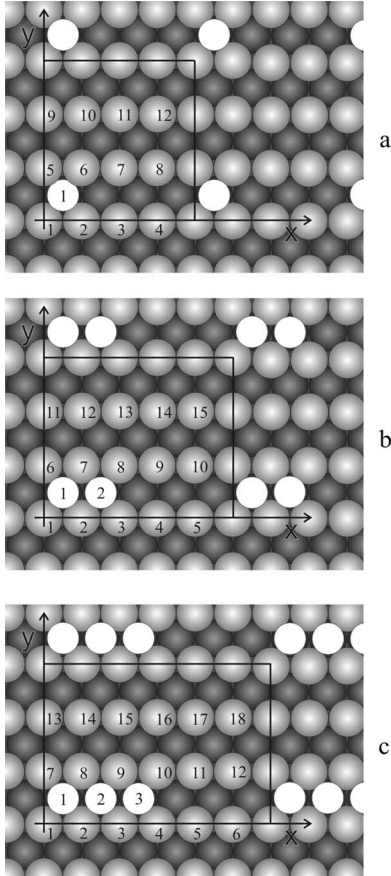


FIG. 3. Adsorption structures for (a) a single Co adatom,  $p(4 \times 3)$ , (b) a dimer,  $p(5 \times 3)$ , and (c) a trimer,  $(6 \times 3)$  on the Cu(110) surface. The calculation supercells are indicated by a rectangle ( $x=[\bar{1}10]$  and  $y=[001]$ ).

as well as with *ab initio* value  $\Delta_{12} = -3.0\%$  (Ref. 8) while the experiments give the small expansion of the second interlayer spacing. On Cu(110), the contraction of the topmost interlayer spacing is bigger than that on Cu(111) and Cu(001) due to lower packing of this surface; while the contraction of the second interlayer spacing is smaller than that in the previous cases. Relative contractions found,  $\Delta_{12} = -2.90\%$  and  $\Delta_{23} = -0.02\%$ , are smaller than those obtained by using high-energy ion-scattering (HEIS) (Ref. 60) ( $\Delta_{12} = -5.3\%$  and  $\Delta_{23} = 3.3\%$ ) and LEED (Ref. 61) ( $\Delta_{12} = -7.9\%$  and  $\Delta_{23} = 2.4\%$ ). Despite some discrepancies in the layer relaxation with available experimental results, the Cu-Cu potentials give surface phonon modes in good agreement with helium atom scattering and electron energy-loss spectroscopies data (see subsection B, Vibrations)

To simulate a single Co adatom on the Cu(111) surface we used  $(3 \times 3)$  and  $(4 \times 4)$  unit cells that correspond to coverages  $\Theta = 1/9$  ML and  $\Theta = 1/16$  ML, respectively (see Fig. 1(a) where the  $(3 \times 3)$  unit cell is shown). A Co adatom was placed at fcc hollow site as it is slightly more preferable than hcp one. The equilibrium distance  $d_{\text{Co-Cu}}$  between the Co adatom and the nearest-neighbor substrate atom was found to be 2.458 Å. Relaxation results in rearrangement of the substrate atoms, especially in the close vicinity of the adatom. Thus, the Cu atoms which are the first nearest neighbors

(NN) to the adatom [atoms 1, 2 and 4 in Fig. 1(a)] have two times larger inward relaxation than the clean Cu(111) surface atoms have. At the same time in the plane they move away from the adatom by 0.012 Å. An atom 5 which is the second-nearest neighbor to the Co adatom shows the outward relaxation and in the plane it moves toward the adatom position by 0.015 Å. Atoms 3 and 7 are the third NNs to Co, they do not show the in-plane displacements and their perpendicular relaxation is almost the same as on the clean surface.

In Fig. 1(b) the simplest adsorbate cluster, dimer, on Cu(111) is shown. The two Co atoms were initially placed at the nearest fcc hollow sites on Cu(111) in the  $(4 \times 4)$  unit cell. Such a big unit cell prevents direct interaction between two dimers in any direction. After relaxation the dimer length was found to be 2.295 Å that is 8.5% shorter than the NN distance in bulk Co. The shortening of the dimer length by 0.263 Å moves atoms of the dimer from the ideal threefold hollow positions, however, the relaxation of the NN substrate atoms accommodates them to restore approximately threefold coordination of the adsorbate atoms. In this case the first NN atoms can be classified into two groups. The first one is formed by atom 2 which is NN to both Co adatoms (NN-2Co) and the second group is formed by atoms 1, 3, 5, and 6 which have only one NN Co adatom (NN-1Co). The  $d_{\text{Co-Cu}}$  distance between Co and the NN-2Co atom has been found to be of 2.470 Å and the distance between Co and NN-1Co atoms has been obtained to be of 2.509 Å. Similar to the case of a single adatom, the second NN atoms move toward the adatom positions by 0.021 Å.

To simulate a cluster of three Co atoms the  $(4 \times 4)$  unit cell has been used. We have also checked the obtained results for the  $(5 \times 5)$  unit cell and found essentially the same results. The Co atoms have initially been placed at three fcc sites on Cu(111) in two different geometries: a triangle and a chain. The molecular-dynamics relaxation of a trimer leads to an equilateral triangle as the most stable configuration [Fig. 1(c)] with the bond length of 2.368 Å that is shorter than the initial one but 0.039 Å longer than that in the free cluster. The shortening of bond length in comparison with its unrelaxed value is provided by displacements of Co adatoms from the initial positions in the direction to the center of gravity of the cluster by 0.110 Å. The alteration of the Co positions is accompanied by displacements of the first and second NN atoms of the substrate. Like to the previous case there are two kinds of the first NN atoms: NN-2Co (atoms 2, 5, 6) and NN-1Co (atoms 1, 3, 9). The in-plane displacements toward the center of the triangle are 0.004 and 0.002 Å for the first and second group atoms, respectively. The vertical displacements of these atoms are  $-0.069$  and  $0.002$  Å, respectively, from their relaxed clean surface positions. As a result the  $d_{\text{Co-Cu}}$  distance for NN-2Co and NN-1Co atoms has been found to be 2.496 and 2.536 Å, respectively. The relaxation of the second NN atoms has been found to be similar to that in the previous cases.

For a single Co adatom on Cu(001) the equilibrium distance  $d_{\text{Co-Cu}}$  between the Co adatom and nearest-neighbor substrate atoms has been obtained equal to 2.476 Å that is slightly longer than the corresponding  $d_{\text{Co-Cu}}$  at Cu(111). The first nearest neighbors to the Co adatom [atoms 1, 2, 4 and 5

in Fig. 2(a)] show inward (vertical) relaxation which is bigger than that of the clean Cu(001) surface by a factor of 1.5. In plane, these atoms move away from the adatom by 0.018 Å. Atoms 3, 6, 7 and 8 (the second NNs to the Co adatom) undergo inward relaxation which is slightly smaller than that for the surface layer atoms at the clean surface. Contrary to the case of a single Co adatom on Cu(111) where the second NN atoms move toward the adatom, on Cu(001) these atoms do not undergo lateral displacements. The third neighbor atom (9) undergoes displacements qualitatively similar to those of the clean Cu(001) surface atoms.

On Cu(001) we analyzed two possible dimer geometries. The first one consist of two Co adatoms placed at the nearest-neighbor fourfold hollow sites and the second dimer was placed at the second-nearest-neighbor hollow sites. The first dimer has been found energetically more favorable by 0.791 eV [see Fig. 2(b)]. The equilibrium dimer length is of 2.326 Å that is 1.4% longer than the Co dimer length on Cu(111). Similar to the case of a dimer on Cu(111) the first NN atoms can be separated in two groups. The first group is of atoms 2 and 6 which are NNs to both Co adatoms (NN-2Co) and the second one is of atoms 1, 3, 5, and 7 which have only one NN Co adatom (NN-1Co). The equilibrium distance  $d_{\text{Co-Cu}}$  between the Co adatom and the NN-2Co atom is of 2.483 Å while the distance between Co and NN-1Co atoms is of 2.528 Å, i.e., one can see the same trend as for the Co dimer on Cu(111) where the NN-2Co atom is located closer to Co than the NN-1Co one. The NN-2Co atoms undergo significant relaxation displacements. In plane, they move away by 0.044 Å in the direction perpendicular to the dimer and show inward relaxation which is 2.7 larger than that on clean Cu(001). The NN-1Co atoms undergo only minor lateral and vertical relaxation.

To simulate a trimer on Cu(001) we considered two different geometries. The first one was a chain of Co adatoms and the second trimer, shown in Fig. 2(c), was placed as a triangle. After relaxation the triangle configuration of adatoms has been found more stable by 0.987 eV than the chain. Contrary to the case of a trimer on Cu(111), where adatoms form an equilateral triangle, a triangle on Cu(001) is isosceles, i.e., it has two different lengths. The equilibrium lengths  $d_{\text{Co}_1\text{-Co}_2(\text{Co}_2\text{-Co}_3)}$  and  $d_{\text{Co}_1\text{-Co}_3}$  were found to be of 2.328 and 2.794 Å, respectively. As one can see the short length is nearly equal to the dimer length. The long length which is equal to the Cu lattice constant before relaxation becomes 0.823 Å shorter after relaxation. Thus, initially right triangle shape cluster tends to be isosceles triangle one. This trend conflicts with the symmetry of the substrate and result in a complicated relaxation of the nearest-neighbor substrate atoms. Contrary to the case of a trimer on Cu(111), where only two kinds of the NN substrate atoms (NN-1Co and NN-2Co) exist, on Cu(001) more complicated geometry of nearest-neighbor Cu atoms arises: five groups of the NN atoms with different relaxations are revealed. The first group is of atoms 1 and 11 which can be characterized by the large (0.091 Å) outward relaxation in the  $z$  direction and by the largest distance (2.683 Å) to the nearest adatom compared to the other NN atoms. The second group consists of one atom (6) only which undergoes huge (−0.242 Å) inward relaxation due to shortening the long bond length of the cluster. This atom has

the shortest distance to the nearest Co atoms (2.420 Å). Other groups are: Cu<sub>2</sub> and Cu<sub>7</sub>; Cu<sub>3</sub>; Cu<sub>5</sub> and Cu<sub>10</sub>. All these atoms have approximately equal inward relaxation, however, they are located at distinct distances from the nearest Co adatoms (in the range of 2.488–2.519 Å) due to different lateral relaxations. Moreover, atoms 2 and 7 have the two NN Co atoms and are situated at different distances from the Co<sub>2</sub> and Co<sub>1(3)</sub> atoms (2.488 and 2.584 Å, respectively).

Contrary to the case of a single Co adatom on close-packed surfaces, on Cu(110) a nearest to the adatom is the second layer Cu atom lying beneath the adatom. It relaxes inward by 0.065 Å due to the Co adsorption and is situated at a distance of 2.448 Å from the adatom. However, for convenience, as before, we will designate the first layer Cu atoms closest to the adatom as the nearest-neighbor atoms. The equilibrium distance  $d_{\text{Co-Cu}}$  between the Co adatom and the nearest-neighbor substrate atoms has been obtained equal to 2.493 Å that is slightly longer than the corresponding  $d_{\text{Co-Cu}}$  at Cu(111) and Cu(001). The first nearest neighbors to the Co adatom [atoms 1, 2, 5, and 6 in Fig. 3(a)] show small inward relaxation (−0.003 Å). In plane, these atoms move away from the adatom by 0.018 Å. Atoms 3, 4, 7, and 8 (the second-nearest neighbors to the Co adatom) undergo small outward relaxation (0.007 Å). The third (9, 10) and fourth (11, 12) neighbor atoms undergo displacements qualitatively similar to those on the clean Cu(110) surface.

On Cu(110) we analyzed two possible dimer orientations: the first one along the  $[\bar{1}10]$  direction [in Fig. 3(b) it corresponds to the  $x$  axis] and the second one along the  $[001]$  direction [in Fig. 3(b) it corresponds to the  $y$  axis]. We have found that the first orientation is lower in energy by 0.827 eV. The equilibrium dimer length is of 2.329 Å that is close to the dimer bond length on Cu(001). The shortest Co–Cu bond length, 2.476 Å, between the adatom and the underlying Cu second layer atoms is slightly longer than that in the single adatom case. As before, the first layer substrate atoms can be separated in two groups. The first group is of atoms 2 and 7 which are NN to both Co adatoms (NN-2Co) and the second group is of atoms 1, 3, 6, and 8 which have only one NN Co adatom (NN-1Co). The equilibrium distance  $d_{\text{Co-Cu}}$  between the Co adatom and the NN-2Co atom is of 2.505 Å while the distance between Co and NN-1Co atoms is of 2.543 Å. The NN-2Co atoms undergo significant lateral and vertical relaxation displacements while the NN-1Co atoms undergo only minor relaxations due to the Co dimer adsorption.

To simulate a trimer on Cu(110) we considered two different geometries. The first one was a chain of Co adatoms along  $[\bar{1}10]$  and the second one was a triangle with the legs along the  $[\bar{1}10]$  and  $[001]$  axes. After relaxation the chain geometry of adatoms has been found to be more stable by 0.943 eV than the triangle one. This clearly shows that the Co<sub>3</sub> cluster on Cu(110) forms a structure distinct from that of free Co<sub>3</sub> [as well as from Co<sub>3</sub> on Cu(111) and on Cu(001)]. This is a consequence of the Co-Cu interactions which can produce the trimer vibrations very distinct from those of free Co<sub>3</sub>.

The calculated equilibrium length  $d_{\text{Co}_1\text{-Co}_2(\text{Co}_2\text{-Co}_3)}$  = 2.375 Å is 0.046 Å longer than that in the dimer on (110).

Similar to the dimer case the shortest distance  $d_{\text{Co-Cu}}$  has been found between the Co atoms and the second layer Cu atoms lying beneath the adatoms. The equilibrium distances between central Co atom of the chain and its underlying Cu atom is 2.473 Å while the Co-Cu distances in the case of chain end atoms are equal to 2.483 Å, that is the end chain atoms are shifted from the fourfold hollow positions to the center of the chain and lie slightly higher than the central atom. Following the previous cases we will denote the first layer Cu atoms, which are closest to the adatoms, as the NN atoms in spite of that the real NN atoms are the Cu underlying ones. Of the nearest neighbors from the first layer atoms it is possible to pick out those which have only one closest Co adatom (NN-1Co) and those which have two NN Co adatoms (NN-2Co). Here the NN-2Co are atoms 2, 3, 8, and 9. They situated at a distance of 2.546 Å from the central Co atom of the chain and at 2.486 Å from the chain end atoms. Atoms 1, 4, 7, and 10 which are the NN-1Co ones have the Cu-Co bond length of 2.556 Å.

## B. Vibrations

### 1. Clean Cu low-index surfaces

In Fig. 4 we show the calculated local density of states (LDOS) for the surface layer of the clean Cu(111), Cu(001), and Cu(110) slabs in comparison with the bulk Cu. The  $z$ -direction and  $xy$ -plane resolved LDOS are plotted. The evaluated LDOS features are typical for the (111), (001), and (110) fcc metal surfaces.<sup>7-9</sup> The prominent peak at 13.65 meV on Cu(111) corresponds to the Rayleigh mode. The obtained vibrational energies for the Rayleigh mode at the high-symmetry points  $\bar{M}$  (13.52 meV) and  $\bar{K}$  (14.84 meV) agree well both with experimental data<sup>62,63</sup> [13.3 (Refs. 62 and 63) and 14.0 (Ref. 63) meV, respectively] and *ab initio* results (13.5 and 15.3 meV).<sup>8</sup> The in-plane polarized vibration peak at 27 meV corresponds to the shear-horizontally polarized surface mode at the  $\bar{M}$  point. This frequency is in a good agreement with *ab initio* calculation results (27.7 and 27.3 meV, for a review see Ref. 8). On Cu(001) more features are seen than on Cu(111). The lowest peak on Cu(001) corresponds to the shear horizontally polarized mode  $S_1$  with a frequency of 9.10 meV at the  $\bar{X}$  point. This frequency value agrees well with *ab initio* calculation results, 9.1–9.9 meV.<sup>8</sup> The highest frequency corresponds to the in-plane polarized mode  $S_6$  at  $\bar{X}$ . The frequency value of this mode, 26.14 meV is in fairly good agreement with *ab initio* calculation data, 23.8–26.1 meV.<sup>8</sup> The vertically polarized lower frequency mode is the Rayleigh wave at  $\bar{X}$  with a frequency of 12.57 meV which is close to *ab initio* results, 12.8–14.0 meV (Ref. 8) and EELS value 13.4 meV.<sup>64</sup> The higher frequency  $z$ -polarized mode peak is the contribution from the Rayleigh mode at the  $\bar{M}$  point. For the (110) surface our results reproduce the dispersion of RW mode, the  $\bar{X}$  gap state and the  $\bar{\Gamma}$  resonance frequencies measured by using HAS.<sup>65</sup> The frequencies of all the obtained surface states are also in a good agreement with *ab initio*<sup>8</sup> and embedded atom method (EAM) (Ref. 7) calculation results.

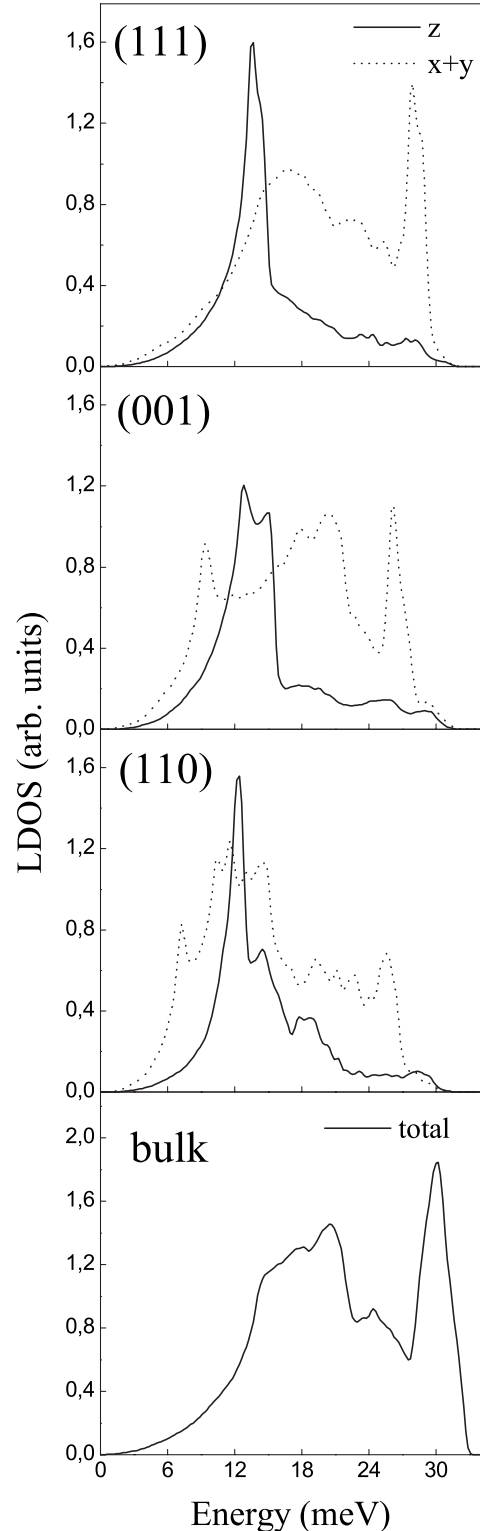


FIG. 4. Local density of vibrational states for the clean Cu(111), Cu (001), and Cu(110) surfaces compared to the bulk DOS.

Summarizing the obtained results one can note that the semiempirical potentials used in the present work provide a good description of surface vibrations on the low-index Cu surfaces.

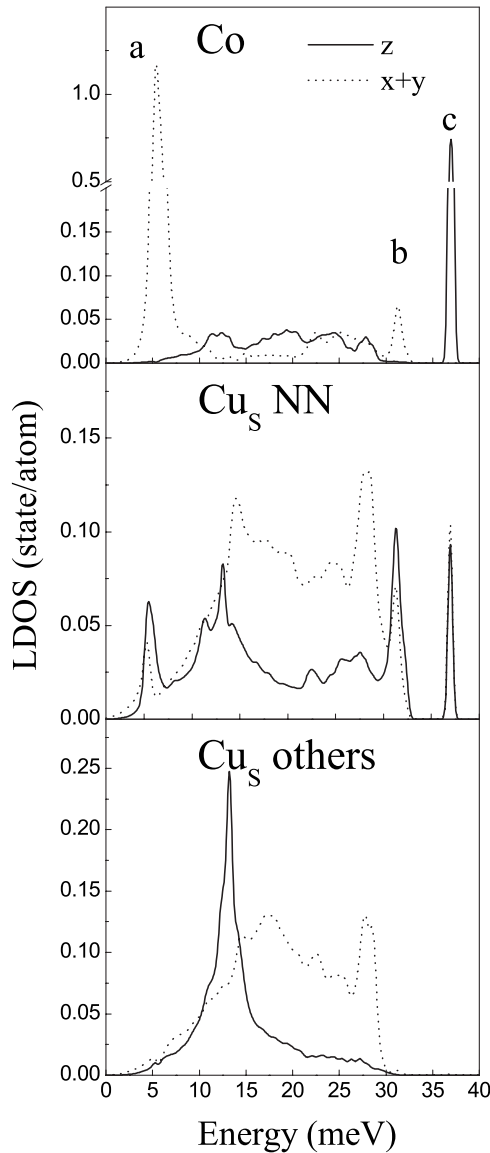


FIG. 5. Local density of vibrational states for a Co adatom on the Cu(111) surface, for the nearest neighbors from the substrate first layer atoms ( $\text{Cu}_s$  NN) and for the rest atoms of the first Cu layer ( $\text{Cu}_s$  others).

### 2. A single Co adatom on the Cu(111) surface

In Fig. 5 the calculated local density of vibrational states is presented for a single Co adsorbate, Cu atoms (1, 2, and 4), nearest neighbors ( $\text{Cu}_s$  NN) to the adatom, and for rest Cu atoms ( $\text{Cu}_s$  others) of the surface layer. Three peaks at 5.38, 31.34, and 36.98 meV originated from the adsorbate vibrations are clearly seen in the figure. The lower frequency peak, (a), as well as the peak b, corresponds to vibrations of the Co adatom in the plane parallel to the surface. The highest frequency peak, (c), is determined by vertical vibrations of the adsorbate. All these adsorbate modes are coupled to the  $\text{Cu}_s$  NN atoms motion causing complicated vibrations of these atoms (see Fig. 6 and the middle panel of Fig. 5) in the vertical and  $x, y$  directions simultaneously. One can note that the vibrations of the  $\text{Cu}_s$  second and third NN atoms are

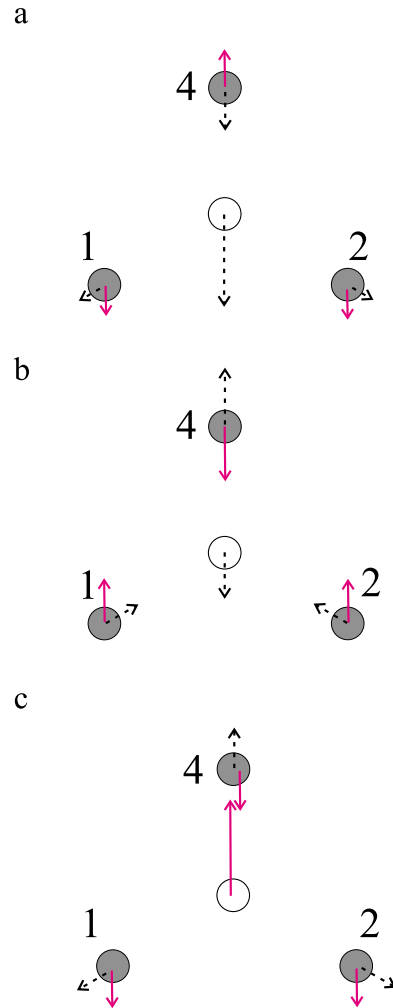


FIG. 6. (Color online) The polarization distributions for modes indicated in Fig. 5 by letters a, b, and c. The gray circles denote the Cu atoms in the first layer, the white one represents the Co adatom. The length of the arrows represent the amplitudes of parallel and perpendicular components of the displacement vectors. Solid pink arrows correspond to the vertical component of the displacements of the atoms and dash arrows display the in-plane component of the vibration vectors. Numbers at the Cu atoms correspond to Fig. 1(a).

mostly coupled to the clean Cu surface vibrational modes that is illustrated in the lower panel of Fig. 5. This demonstrates a short-range effect of the Co adatom interaction with the Cu substrate.

Vibrations of a single Co adatom on Cu(111) have recently been studied by Liu and Gao<sup>40,41</sup> by using the VASP *ab-initio* code and semiempiric many-body potentials. The frequencies and polarizations obtained by Liu and Gao are in excellent agreement with our results except the peak b which was missed in Refs. 40 and 41. Taking into account that Liu and Gao used in their calculations<sup>41</sup> the similar many-body potentials,<sup>30</sup> we attribute the discrepancy with our results to different details of the calculations. In particular, Liu and Gao used an 11-layer Cu substrate instead of 31-layer film we use. Another possible reason for missing the peak b might be the use not sufficiently big number of  $\mathbf{k}$  points for the LDOS calculation.

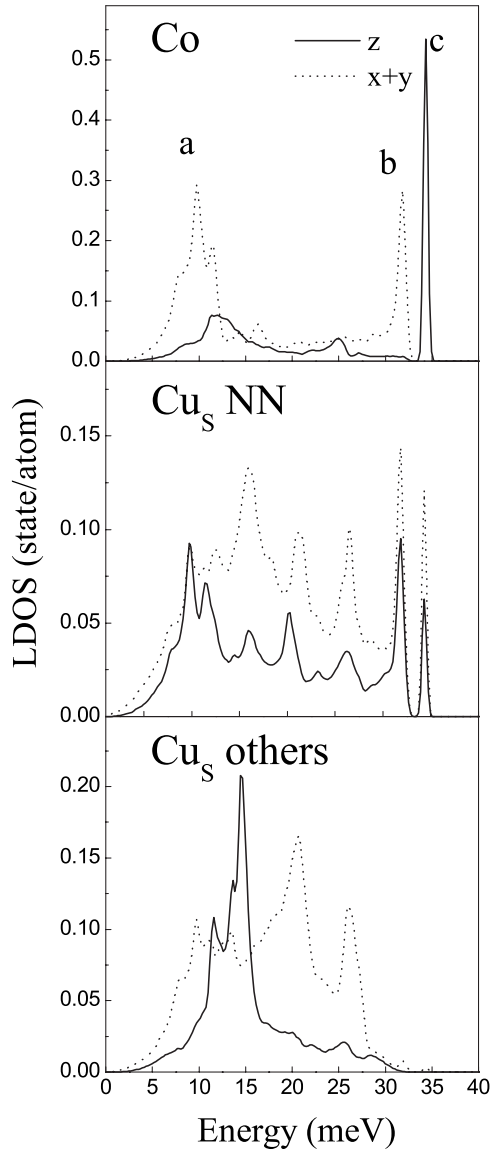


FIG. 7. Local density of vibrational states for a Co adatom on the Cu(001) surface, for nearest neighbors from the substrate first layer atoms ( $\text{Cu}_s$  NN), and for second and third nearest-neighbor atoms from the first Cu layer ( $\text{Cu}_s$  others).

The final width of the Co LDOS peaks  $a$ ,  $b$ , and  $c$  is caused by coupling of these modes to the substrate vibrations. The respective lifetimes are of 0.63, 0.68, and 1.47 ps for the  $a$ ,  $b$ , and  $c$  Co vibrational modes, respectively. The longer lifetime of the  $c$  mode is accounted for by location of this mode above the bulk Cu spectrum. This location leads to coupling of the Co adatom motion to vibrations of the Cu atoms from the surface layer only while the modes  $a$  and  $b$  are coupled to motion of both the surface and bulk Cu atoms.

### 3. A single Co adatom on the Cu(001) surface

In Fig. 7 we show the calculated local density of vibrational states for a single Co adatom, for the first NN Cu atoms (atoms 1, 2, 4, and 5), and the rest Cu atoms ( $\text{Cu}_s$  other) of the Cu(001) surface layer. As one can see there are three sharp peaks in the Co originated LDOS. The lower one

( $a$ ), similar to the case of Co on Cu(111), corresponds to the in-plane motion of Co. Nevertheless, there are two important differences. The frequency of this vibration (9.72 meV) is significantly higher and the peak width is wider than that on Cu(111). Both these features are naturally explained by stronger interaction of the Co atom with the  $\text{Cu}_s$  NN atoms in comparison with the case of Co/Cu(111). However, the complex structure of the peak reflects non-negligible interactions with the other  $\text{Cu}_s$  atoms of the surface layer. The second peak ( $b$ ) also corresponds to the in-plane vibrations of adatom. This vibration with a frequency 31.85 meV is similar to that at 31.34 meV for Co on Cu(111). In contrast to the peak ( $a$ ), the peak ( $b$ ) is narrower due to interaction of Co mainly with the  $\text{Cu}_s$  NN atoms of the surface layer. The third peak ( $c$ ) is the vertically polarized vibration of the Co atom. Due to strong interaction of Co with the  $\text{Cu}_s$  NN atoms, the latter is involved in the complex vibration in the  $z$  and  $x,y$  directions. The frequency of this mode, 34.33 meV, is approximately 3 meV smaller than that for a single Co adatom on Cu(111). However, despite this decrease the  $c$  mode frequency is still higher than the entire bulk Cu spectrum. This position explains the calculated long lifetime, 1.43 ps, of the vertical Co mode which is very close to that for the  $c$  mode of Co on Cu(111). The obtained lifetime value of the  $b$  mode, 0.68 ps, is equal (accidentally) to that of the  $b$  mode for Co/Cu(111). In contrast, the lifetime of the  $a$  mode (central peak of the  $a$  complex structure), 0.31 ps, is shorter by a factor of 2 than that of the  $a$  mode for Co on Cu(111). The very short lifetime of the latter mode is accounted for by the interaction of the Co vibration with surface and bulk Cu atoms vibrations (qualitatively it is easily seen from the overlap of the  $a$  mode frequency with the bulk Cu phonon spectrum).

### 4. A single Co adatom on the Cu(110) surface

In Fig. 8 the calculated local density of vibrational states is presented for a single Co adatom, for the substrate second layer atom, ( $\text{Cu}_{13}$ ), lying beneath the adatom, and for the first NN Cu surface layer atoms (atoms 1, 2, 5 and 6). As one can see, like for the adatom on Cu(001), there are three sharp peaks in the Co originated LDOS. Peaks ( $a$ ) at 6.33 meV and ( $b$ ) at 33.63 meV corresponds to the in-plane motion of the Co atom. The polarizations of these vibrations are quite similar to those for Co/Cu(001), however, the frequencies are shifted in comparison with Co/Cu(001) due to anisotropy of the adatom-substrate interaction in the  $x$  and  $y$  directions on the (110) surface. The third peak ( $c$ ) at 36.11 meV is the vertically polarized vibration of the Co atom. This mode has the higher frequency than the corresponding  $z$ -polarized vibration of Co on Cu(001) and is provided by interaction with distinct substrate atoms. Contrary to the Co/Cu(001) case where the  $z$  peak is originated from the interaction of adatom with the Cu first layer NN atoms, for Co/Cu(001) it is the result of strong interaction of Co with the second layer Cu atom lying beneath the adatom.

The lifetime of the  $a$  mode has been estimated as 0.55 ps that is slightly distinct from the corresponding low-frequency mode  $a$  on Cu(111) and Cu(001). The broadening of the  $b$  mode is significantly smaller on Cu(110) due to the position

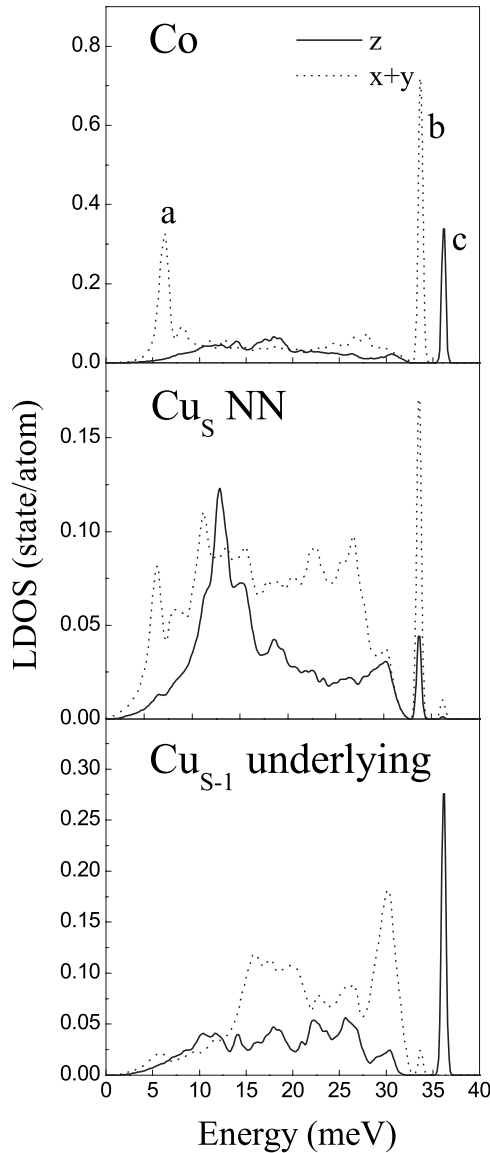


FIG. 8. Local density of vibrational states for a Co adatom on the Cu(110) surface, for nearest neighbors from the substrate first layer atoms ( $\text{Cu}_s$ , NN) and for the second layer atom which lies beneath the adatom (the lower panel).

of this mode above the entire bulk Cu spectrum. The respective lifetime has been found to be of 1.48 ps. The calculated lifetime of the  $z$ -polarized mode  $c$ , 1.59 ps, is comparable with that for a single Co adatom on Cu(111) and Cu(001).

### 5. Free Co clusters

In this subsection, before discussing vibrations of the Co dimer and trimer on the Cu surfaces, we briefly analyze vibrations of the unsupported (free) Co clusters. A free dimer has 6 degrees of freedom, of them only one corresponds to vibrational, optical-like, mode with atomic motion along the dimer axis. In equilibrium, the free Co dimer vibrates with a frequency of 36.48 meV. This result is in excellent agreement with photoelectron spectroscopy data  $34.74 \pm 2.50$  meV and 36 meV obtained by Leopold and Lineberger<sup>66</sup> and by

DiLella *et al.*,<sup>67</sup> respectively. *Ab initio* calculations of  $\text{Co}_2$  vibrations<sup>51</sup> give values in the range 52–55 meV which are 50% higher than our computation frequency while a lower vibrational energy of 29.3 meV is obtained from the TBHH evaluation.<sup>52</sup>

A free equilateral triangle shape trimer has 9 degrees of freedom, of which only three correspond to vibrational modes. The highest frequency mode, 36.36 meV, of  $\text{Co}_3$  is symmetric (optical-like) mode with a fixed center of gravity at the center of equilateral triangle. As one can see the energy of this vibration just slightly lower of that for the stretch mode of the dimer. The lower, degenerate (because of  $C_{3v}$  symmetry) frequency mode of 25.77 meV is characterized by deformational and antisymmetric vibrations of the cluster. We have also computed vibrations of the isosceles shape  $\text{Co}_3$  clusters which are of  $C_{2v}$  symmetry with two long (2.36 Å) and one short (2.26 Å) sides as well as with two short (2.30 Å) and one long (2.40 Å) sides. The difference of 0.1 Å between the length of the long and short sides we used as typically obtained from *ab initio* calculations. The reduction of symmetry from  $C_{3v}$  to  $C_{2v}$  leads to slight increase to  $\approx 38$  meV of the higher frequency to slight splitting of the lower degenerate mode,  $\approx 22$  and 28 meV.

The energies of vibrational modes of  $\text{Co}_3$  were calculated by using *ab initio*<sup>51</sup> and TBHH (Ref. 52) theories. The energy of the symmetric stretch mode was found by Castro *et al.*<sup>51</sup> to be of 49.6 and 45.2 meV in local spin-density approximation (LSDA) and generalized-gradient approximation (GGA) approaches, respectively, while it was obtained to be of 28.1 meV in Ref. 52. As in the case of  $\text{Co}_2$  these data, respectively, overestimate<sup>51</sup> and underestimate<sup>52</sup> our stretch mode energy. The same trend is for two lower energy vibrations.

A free chain of three atoms has four vibrational modes. Two degenerated deformational modes have frequencies close to zero. The highest frequency mode, 39.98 meV, of the Co chain trimer is antisymmetric one. The lower frequency mode of 25.34 meV is characterized by symmetric vibrations with a fixed center of gravity. Both these energies are quite close to those of the respective vibrations of both equilateral and isosceles triangles of Co.

### 6. A Co dimer on Cu(111)

In Fig. 9 we show the calculated local density of states for the Co dimer atoms and for the first Cu layer NN atoms. As was mentioned before, these NN atoms can be classified in two groups. The first group consists of one atom only [atom number 2 in Fig. 1(b)] which has two Co adatoms as the nearest neighbors (NN-2Co) with  $d_{\text{Co-Cu}}=2.470$  Å. The second group is of atoms 1, 3, 5, and 6. Each of these atoms has only one nearest Co atom (NN-1Co) with  $d_{\text{Co-Cu}}=2.509$  Å. Contrary to the single adatom case, LDOS for the Co dimer on Cu(111) shows two low-frequency peaks which correspond to vibrations of the cobalt atoms in the plane parallel to the surface. The first peak, ( $a$ ), at 4.47 meV is a degenerate vibrational state with two kinds of vibrations ( $a1$  and  $a2$  in Fig. 10). The  $a2$  vibration is the frustrated rotation mode that corresponds to rotatory vibration of the dimer relative to its center of mass, and the  $a1$  vibration is characterized by

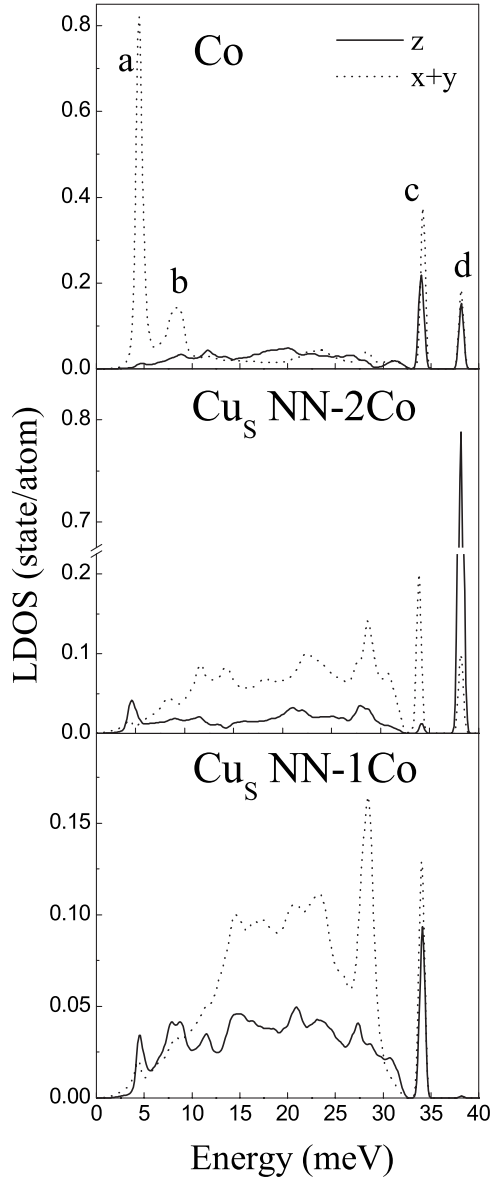


FIG. 9. Local density of vibrational states for a dimer on the Cu(111) surface and for nearest neighbors from the Cu surface layer (see the text).

displacements of the entire dimer in the direction perpendicular to the dimer axis (frustrated translation mode). The second peak, (*b*), at 8.56 meV corresponds to the entire Co dimer vibration along the dimer bond. As follows from the figure (see the middle and lower panels) all these Co vibrations only slightly involve the NN atoms. The third (*c*) and fourth (*d*) peaks of the Co LDOS at 34.00 and 38.22 meV, respectively, correspond to mixed vibrations of the Co adatoms in the direction perpendicular to the surface and along the dimer bond. The degenerate vibrational mode [peak (*c*)] includes two kinds of the dimer motion, *c1* and *c2*. The *c1* mode is a rotary vibration of the dimer in the plane perpendicular to the surface. Modes *c2* and *d* result from the stretch vibration of the free dimer, however, due to the interaction with the substrate they have an additional vertical component of motion and distinct frequencies because of different bond-

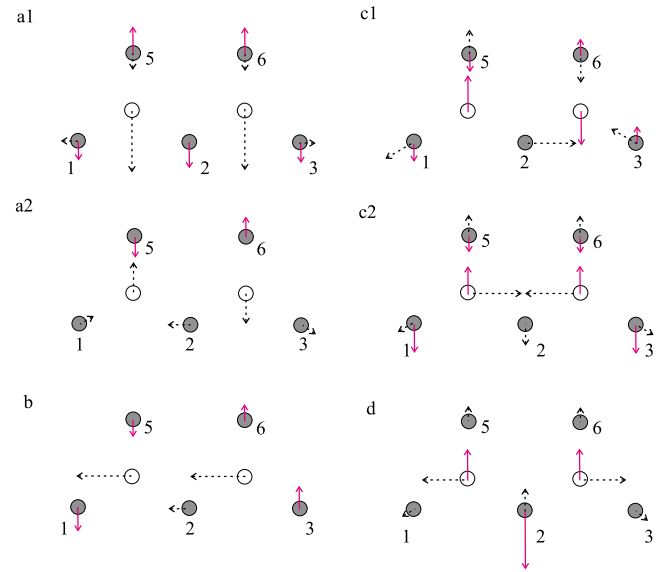


FIG. 10. (Color online) The polarization distributions for peaks indicated in Fig. 9. All the notations are as in Fig. 6.

ing of the Co adatoms with the NN-2Co and NN-1Co atoms. In contrast to the *a* and *b* modes, the Co atoms motion in the *c* and *d* modes strongly couples to the NN substrate atoms motion. In particular, in the *c2*-mode the Co atoms are mainly coupled to the NN-1Co atoms motion, while in the *d* mode, the Co atoms are mostly coupled to the NN-2Co substrate atom motion.

The fitting of the Co LDOS peaks by the Lorentzian function gives lifetimes of 0.93, 0.23, 1.32, and 1.49 ps for the *a*, *b*, *c*, and *d* modes, respectively. The lifetime of the dimer horizontal *a* mode is the longest one compared to the respective *a* mode of a single adatom of Co on all the low index surfaces of Cu. This can be explained by an overlap of this state with a smaller number of bulk Cu states that results from the lower energy (4.47 meV) of the dimer mode. Long lifetimes of the *c* and *d* modes are accounted for by the position of these modes above the bulk Cu spectrum. One can note that in the lifetime estimation of the *c* peak we considered this peak as a sum of the *c1* and *c2* modes taking into account both the vertical and horizontal polarizations. Both the polarizations have also been included in the lifetime estimation of the *d* mode.

### 7. A Co dimer on Cu(001)

More complicated structure of LDOS arises for the Co dimer on Cu(001) (Fig. 11). First of all the low-frequency peaks become wider that indicates that in-plane vibrations are less localized. Contrary to the dimer on Cu(111) where the lowest vibrational mode is degenerate and corresponds to the rotary vibration of the dimer as well as to the vibration of the entire dimer in the plane parallel to the surface in the direction perpendicular to the dimer axis; on Cu(001) the respective peak [at 8.07 meV (*a*)] corresponds to the latter kind of vibration only. It is coupled to the *z*-polarized vibrations of the Cu surface layer atoms. While a peak at 12.9 meV (*b*) corresponds to the dimer frustrated rotation mode

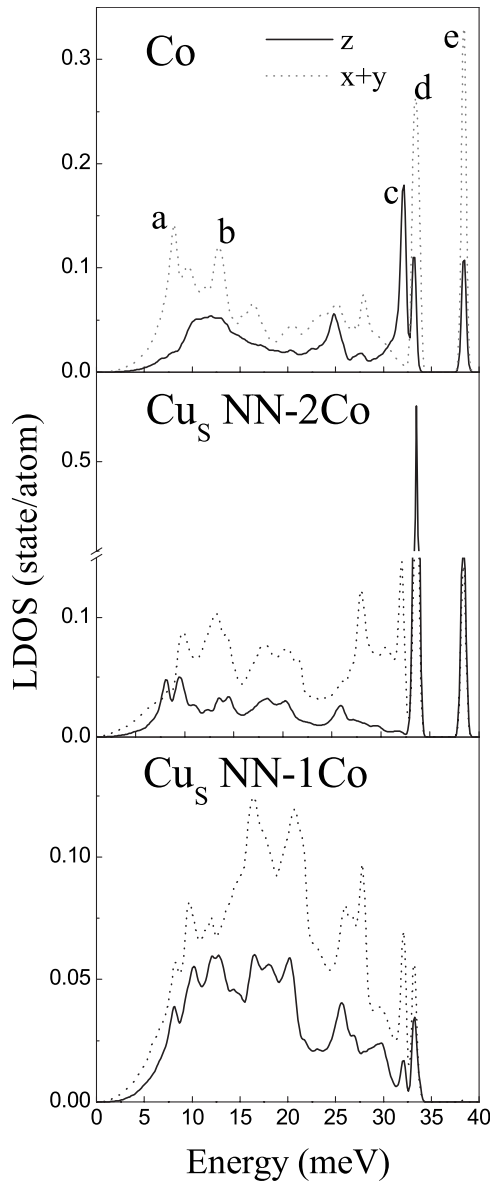


FIG. 11. Local density of vibrational states for a dimer on the Cu(001) surface and for nearest neighbors from the Cu surface layer (see the text).

strongly coupled to vibrations of the NN-1Co atoms as well as to vibrations of the second-nearest-neighbor atoms. The weak peak at 9.5 meV (not denoted in the figure) is associated with vibrations of the entire dimer along the dimer bond. Other peaks in the middle frequency region such as that of 24.82 meV correspond to vibrations of the adatoms strongly coupled to the substrate atoms. In the high-frequency region, contrary to the case of the dimer on Cu(111) where only two modes exist, on Cu(001) we have found three sharp peaks. The first peak (*c* in Fig. 11) at 32.14 meV corresponds to the *z*-polarized vibration of the adatoms in opposite directions (frustrated rotation vibration in the plane perpendicular to the surface) which is coupled to the in-plane vibrations of the NN atoms of the substrate. It is similar to polarization of the *c*1 vibration of the dimer on Cu(111). The next peak corresponds to two modes with fre-

quencies of 33.13 meV (*d*1) and 33.38 meV (*d*2). The first mode is analogous to the *c*2 mode at 34.00 meV for the dimer on Cu(111). It corresponds to vibrations of the Co adatoms in the vertical direction and along the dimer bond. The vibrational mode *d*2 is characterized by strong coupling of the NN-2Co atoms displacements (vertical and in the direction perpendicular to the dimer bond) to the in-plane vibrations of the dimer atoms across the dimer bond. The highest frequency mode, *e*, of 38.46 meV is similar to that of 38.22 meV for the Co dimer on Cu(111). Modes *d*1 and *e* result from the stretching vibration of the free dimer. However, they are split and show additional vertical component of displacements due to interaction with the substrate atoms.

Since the low-frequency spectrum of the Co dimer on Cu(001) is rather broad we estimate vibrational lifetimes only for narrow high-frequency modes *c*, *d*, and *e*. The fitting of these peaks that includes both horizontal and vertical polarizations gives the lifetimes of 0.91, 0.92, and 1.39 ps, respectively. The highest lifetime value of 1.39 ps is accounted for by the position of the mode out of bulk Cu spectrum.

#### 8. A Co dimer on Cu(110)

In Fig. 12 we show the LDOS features for the Co dimer atoms, for the Cu(110) surface layer NN atoms, and for the Cu second layer underlying atoms. In the low and middle frequency regions, the Co vibration peaks are broad, they are even broader than those for the Co dimer on Cu(001). It assumes weak localization of these modes at the dimer atoms. Vibrations *a* and *c* are characterized by translational motion of the entire dimer along the  $[\bar{1}10]$  axis. The Co atoms displacements of the *a* mode are coupled to the motion of the NN atoms in the same direction whereas vibrations of the *c* mode are coupled to displacements of the NN atoms in the opposite direction. The *b* peak at 17.12 meV is originated from the vibration which is absent in the cases of the Co dimer on Cu(111) and Cu(001). This vibration couples the motion of the adatoms and the underlying Cu atoms in the *z* direction. The peak *d* at 31.40 meV corresponds to the rotary vibration of the dimer in the plane parallel to the surface, it is coupled mainly to the NN-2Co and underlying Cu atoms. The peak *e* at 34.34 meV corresponds to three different kinds of vibrations. The first mode, *e*1, is similar to the *d*2 vibration of the dimer on Cu(001). The *e*2 vibration is the stretch in-plane mode with vertical displacements of the entire dimer. This motion is coupled to the *z*-polarized motion of the underlying atoms. The *e*3 mode corresponds to the *z*-polarized vibration of the adatoms in opposite directions such as the *c* mode of the dimer on Cu(001). However, on Cu(110) it is about 2 meV higher than that on Cu(001) due to strong coupling with the underlying atoms motion. The highest frequency mode of 36.11 meV is similar to that of 38.46 meV for the dimer on Cu(001). So, the *e*2 and *f* modes, like to the case of the dimer on Cu(001) and Cu(111), result from the stretch vibration of the free dimer. These modes are split mainly due to strong interaction with underlying Cu atoms (and with Cu atoms 2 and 7 in the case of the *f* mode).

As in the case of the Co dimer on Cu(001) we estimated the lifetimes by Lorentzian fitting only for high-frequency

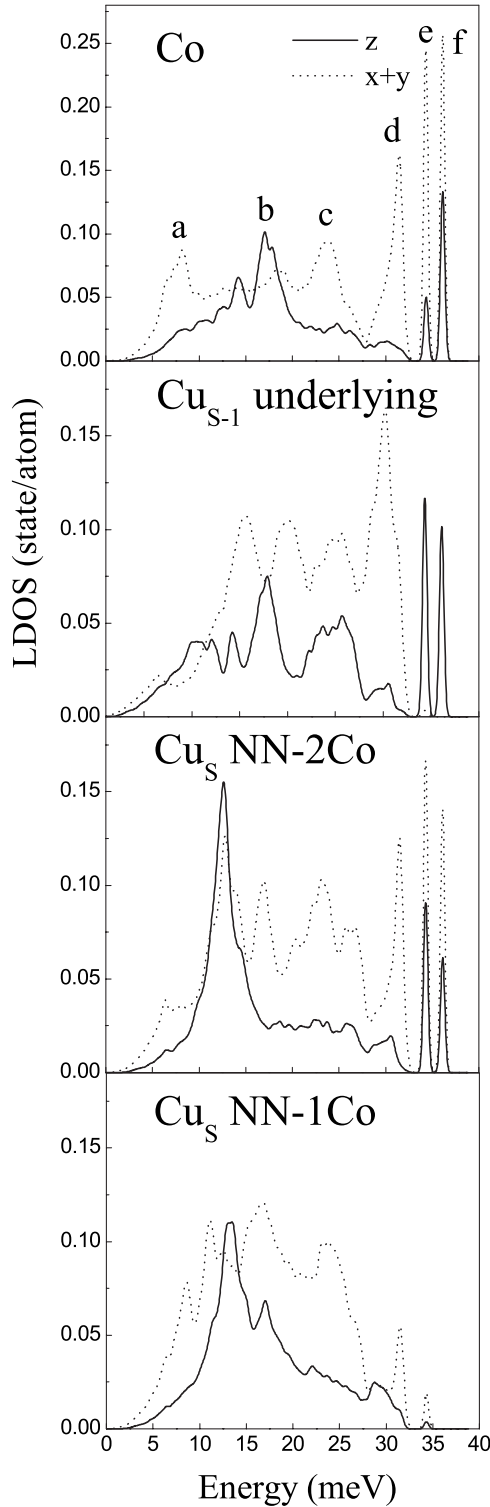


FIG. 12. Local density of vibrational states for a Co dimer on the Cu(110) surface, for nearest neighbors from the Cu surface layer (see the text), and for the Cu second layer atoms which lie beneath the adatoms ( $\text{Cu}_{s-1}$  underlying).

peaks of the Co LDOS. The fitting of the  $e$  ( $e=e_1+e_2+e_3$ ) and  $f$  peaks gives 1.47 ps for both features, while the  $d$  mode shows sufficiently shorter lifetime, 0.28 ps.

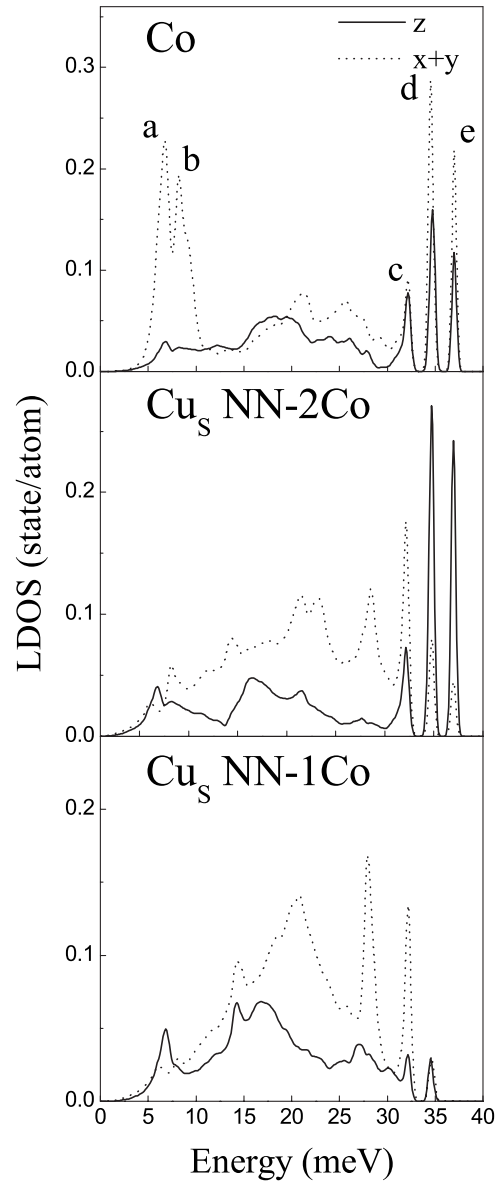


FIG. 13. Local density of vibrational states for a Co trimer on the Cu(111) surface and for NN substrate atoms.

### 9. A Co trimer on Cu(111)

In Fig. 13 we show the LDOS features for the Co trimer atoms and for the Cu(111) surface layer NN atoms. As in the previous cases, LDOS's of NN-1Co (atoms 1, 3, 9) and NN-2Co (atoms 2, 5, 6) atoms are shown separately. In Fig. 14 we show polarization vectors for the Co-induced modes. In the low-frequency region one can see the two peak structure of in-plane vibrations of the adatoms. The lowest frequency peak at 6.70 meV ( $a$ ) corresponds to displacements of the entire cluster and the second one at 8.18 meV ( $b$ ) is the rotary vibration of the cluster relative to its center of mass. These in-plane polarized modes ( $a$  and  $b$ ) are similar to  $a_1$  and  $a_2$  modes found for the dimer on Cu(111). However, contrary to the dimer case where they are degenerate here, the  $a$  and  $b$  modes are split by 1.5 eV. As in the previous cases, the low-frequency in-plane vibrations of Co are

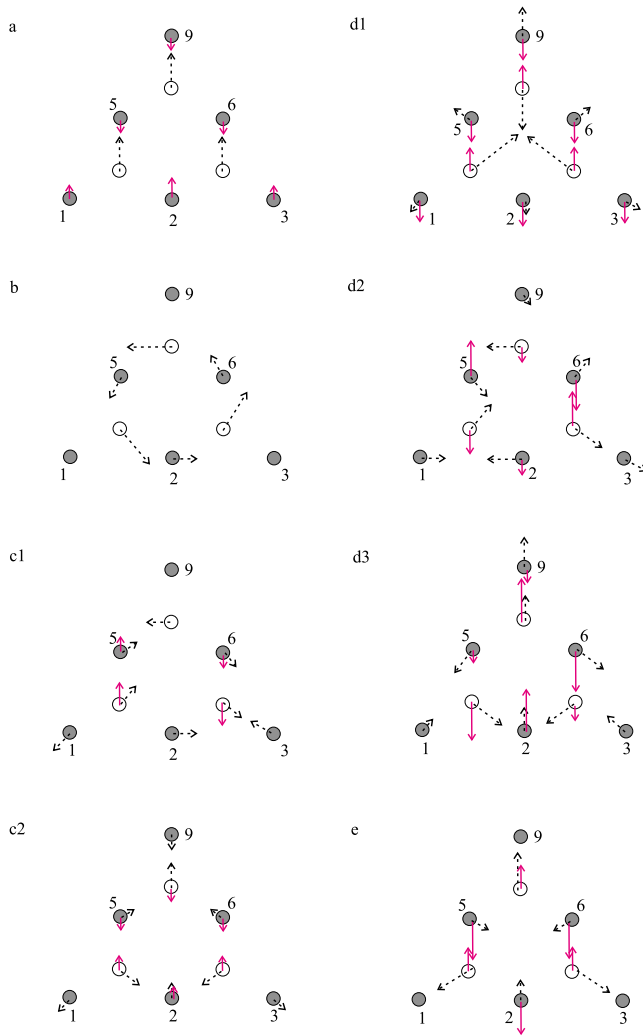


FIG. 14. (Color online) The polarization distributions are shown for peaks indicated in Fig. 13. All the notations are as in Fig. 6.

weakly coupled to vibrations of the substrate atoms while high-frequency Co vibrations which have non-negligible vertical contributions to Co displacements are strongly coupled to the Cu NN atoms vibrations. The peak at 32.14 meV (*c*) is formed by two modes. One of them (Fig. 14, panel *c1*) inherits the antisymmetric vibration from the free Co trimer, while the other mode (Fig. 14, panel *c2*) inherits the deformational vibration from the free trimer. Both these vibrations, being modified by vertical displacements of Co atoms, are strongly coupled to the substrate atom vibrations. The peak at 34.74 meV (*d*) is formed by three modes. The first of these modes (Fig. 14, panel *d1*) is an optical-like in-plane vibration of the Co trimer modified by vertical displacements of the entire trimer. The second and third modes (Fig. 14, panels *d2* and *d3*) are, respectively, antisymmetric and deformational vibrations also modified by vertical motion of the Co trimer atoms. All these modes are coupled to both the Cu NN-2Co and Cu NN-1Co atoms. The highest frequency mode at 36.98 meV (*e*) is an optical-like in-plane vibration of the trimer mixed with vertical displacements of the entire trimer. These Co atoms motions are strongly coupled to the vertical vibration of the entire trimer of the Cu NN-2Co at-

oms modified by optical-like in-plane motion of the latter atoms. One can note that the Cu NN-1Co atoms are not involved in this vibration. So *d1* and *e* vibrations inherit their polarization from symmetrical vibration of the free trimer and are split due to different interaction with NN substrate atoms like a stretch mode of the dimer on Cu(111). The same is true for pairs of antisymmetric and deformational types of vibrations.

The lifetime of the broad *a* and *b* peaks can be estimated as 0.3–0.4 ps. The fitting of the well localized high-frequency peaks gives 0.89, 1.23, and 1.47 ps for the *c* ( $c=c1+c2$ ), *d* ( $d=d1+d2+d3$ ), and *e* peaks, respectively. One should note that highest stretch mode has the lifetime close to that for the dimer and single adatom on the (111) surface.

### 10. A Co trimer on Cu(001)

As follows from Fig. 2, panel *c*, Co atoms 1 and 3 occupy symmetrically equivalent positions with respect to a vertical plane that passes through a Co atom 2 and Cu atoms 3, 6, and 9. This leads to identical LDOS features for Co atoms 1 and 3 (Fig. 15, panel Co-1,3) and to distinct LDOS for Co atom 2 (Fig. 15, panel Co-2). In the lower panels we show LDOS for the first layer Cu NN atoms in ascending order with respect to the Cu-Co distance. Similar to the case of the Co trimer on Cu(111) we have found two peaks in the low-frequency region also for the Co trimer on Cu(001) (see Fig. 15, panel Co-1,3) which are mostly in-plane vibrations of the Co atoms (see Fig. 16, panels *a*, *b1*, and *b2*). In spite of this similarity there exist some distinctions in the character of vibrations. The first one is the absence of the rotary vibration of the cluster. The second distinction which arises from incompatibility of symmetry of an isosceles triangle cluster and the (001) substrate is the polarization of the lowest frequency mode at 4.96 meV (Fig. 16, panel *a*) which is different from any other found in the previous cases. Another low-frequency peak at 8.31 meV (*b*) is a degenerate mode with the in-plane displacements of the entire cluster (Fig. 16, panels *b1* and *b2*).

In the high-frequency region we have found five sharp peaks. These modes differ in polarization from those found for the Co trimer on Cu(111). This is related to different bonding between atoms of the trimer and between the Co atoms and the Cu substrate atoms. The peak at 33.50 meV (*c*) corresponds to the mainly *z*-polarized vibration of the Co-2 atom that is strongly coupled to horizontal motion of Cu atoms 2, 6, and 7 toward the Co-2 atom. This mode resembles the vibration mode (*c*) for the single Co adatom on Cu(001) (Fig. 7). Another difference in the trimer vibrations on Cu(111) and Cu(001) is a splitting of deformational and antisymmetrical trimer vibrations on Cu(001) due to reduction of symmetry of the cluster from  $C_{3v}$  to  $C_{2v}$ . The LDOS peak at 34.74 meV (*d*) corresponds to vibration of the trimer with polarization similar to that for the deformational vibration [if the Cu(001) symmetry is taken into account]. The peak at 37.47 meV (*f*) can be associated with the antisymmetrical vibration of the trimer coupled to the vertical motion of the Co atoms caused by interaction with the substrate. The LDOS peaks at 35.98 meV (*e*) and 41.07 meV (*g*)

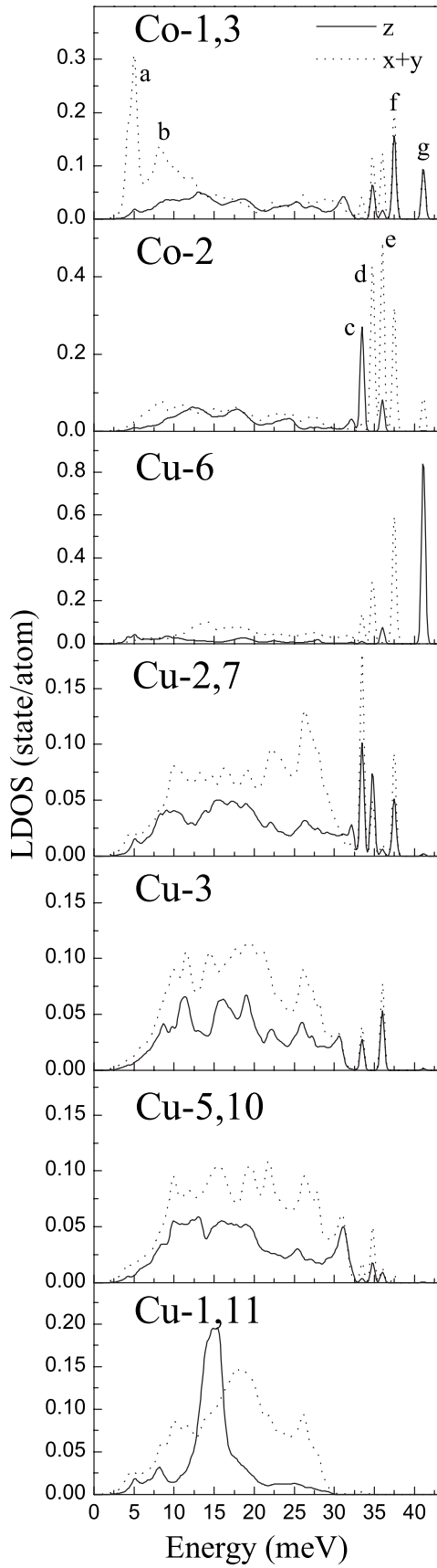


FIG. 15. Local density of vibrational states for a Co trimer on Cu(001) and for NN substrate atoms.

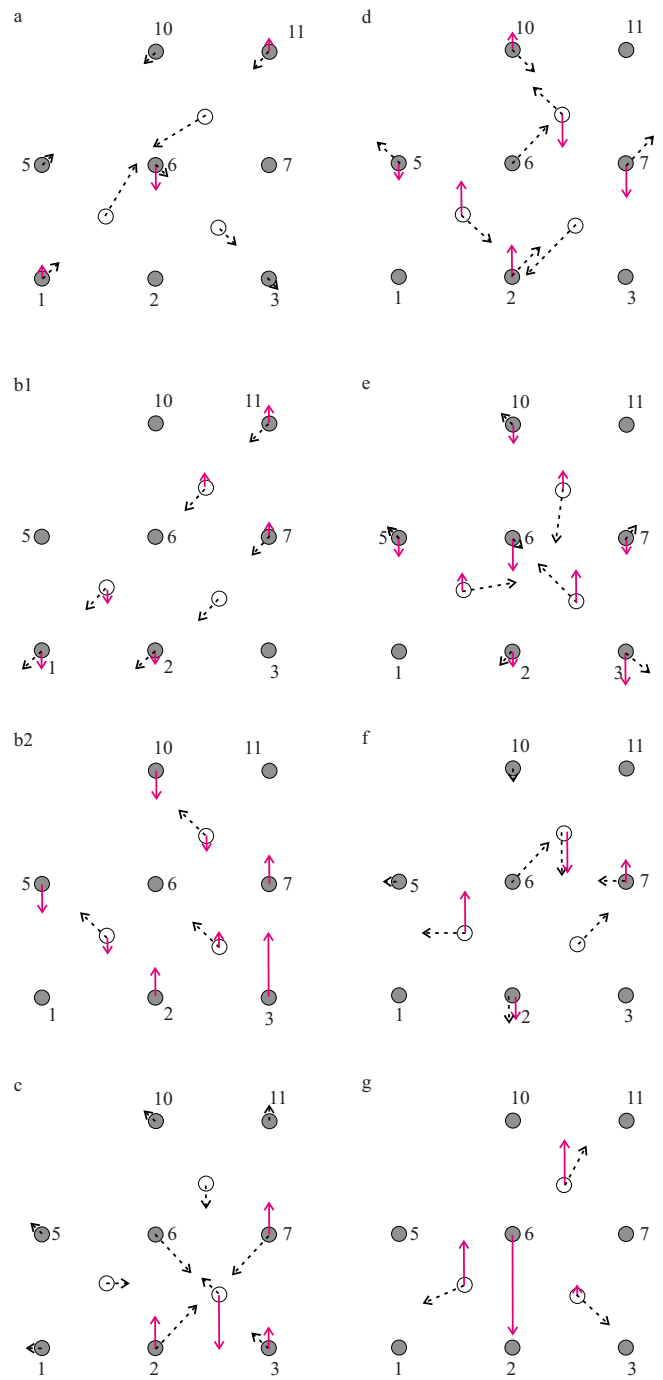


FIG. 16. (Color online) The polarization distributions are shown for peaks indicated in Fig. 15. All the notations are as in Fig. 6.

results from the symmetrical vibration of the trimer with additional vertical contribution to polarization caused by mixing with the substrate NN atoms motion. These modes are similar to those found for the Co trimer on Cu(111).

Here besides the high-energy modes the *a* mode is fairly well localized. The fitting of the *a* peak gives 0.37 ps. Sharp high-frequency peaks *c-g* have nearly identical broadening that leads to lifetimes of 1.40, 1.37, 1.41, 1.40, and 1.39 ps for the *c*, *d*, *e*, *f*, and *g* modes, respectively.

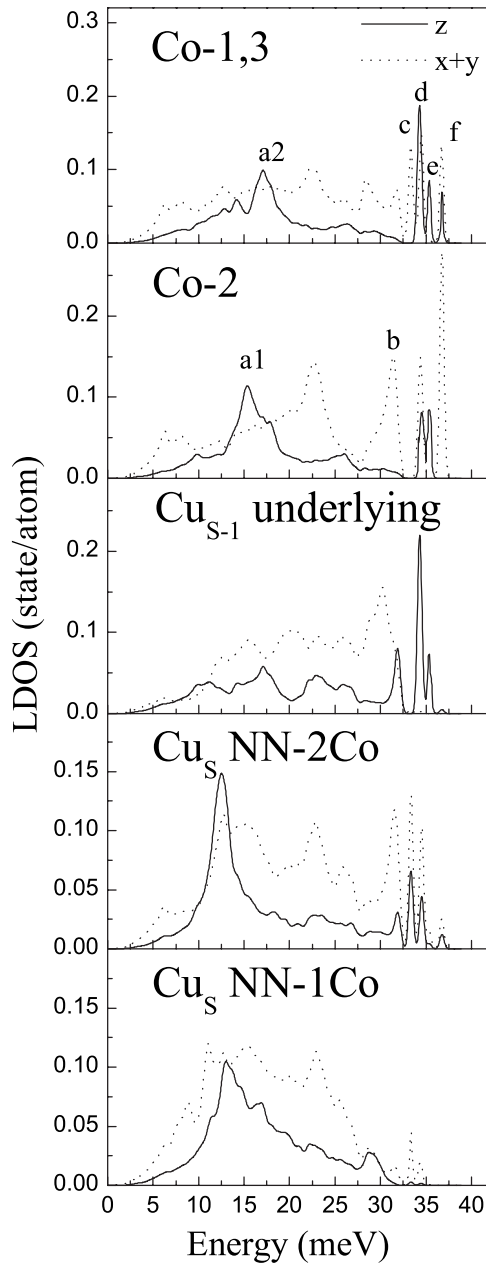


FIG. 17. Local density of vibrational states for a Co trimer on Cu(110) for nearest neighbors from the Cu surface layer (see the text), and for Cu second layer atoms which lie beneath the adatoms ( $\text{Cu}_{s-1}$  underlying).

### II. A Co trimer on Cu(110)

Finally we discuss vibrations of the Co chain trimer on Cu(110). As was reported above the end Co atoms 1 and 3 have distinct positions with respect to the Cu surface plane in comparison with that of the atom 2. They are shifted from fourfold hollow positions to the center of the chain and lie slightly higher than the central atom of the trimer. This difference in positions and bonding of the Co atoms with the substrate atoms leads to small splitting of the  $z$ -polarized vibrations in two peaks of LDOS ( $a1$  at 15.34 meV and  $a2$  at 17.08 meV, Fig. 17). These peaks correspond to the coupled adsorbate—underlying atom vibrations analogous to that de-

termined by the  $b$  peak of the Co LDOS for the dimer on Cu(110). Other weak peaks of the Co LDOS in the low-frequency region are mainly determined by the in-plane translational vibrations of the Co chain mixed with substrate atoms vibrations. In the middle frequency region, some peaks like that at around 22.7 meV have contribution from the in-plane polarized deformational vibrations of the Co chain. The  $b$  peak at 31.4 meV is also formed by deformational and translational vibrations of the trimer. In the high-frequency region we find four sharp peaks. The first of them,  $c$ , at 33.34 meV, is originated from the in-plane rotary vibration of the trimer relative to its center of mass. This mode is similar to the  $d$  mode found for the dimer on Cu(110). Next peak,  $d$ , is formed by three different kinds of vibrations with close frequencies. The  $d1$  vibration with a frequency of 34.30 meV is antisymmetrical vibration of the chain accompanied by vibrations of the first layer NN atoms and mixed with the  $z$ -polarized vibrations of the underlying atoms. The  $d2$  vibration at 34.40 meV is deformational vibration of the chain in the plane perpendicular to the surface strongly coupled to the underlying atom vibration. The  $d3$  mode, such as  $e2$  vibration in the dimer on Cu(110), is caused by strong coupling of the NN-2Co atoms vibrations to the in-plane vibrations of the trimer atoms across the chain axis. Other peaks,  $e$  at 35.31 meV and  $f$  at 36.77 meV are determined by symmetrical ( $e$ ) and antisymmetrical ( $f$ ) vibrations of the chain coupled to the first layer NN and underlying Cu atoms. Thus, the symmetrical mode energy increases by  $\approx 10$  meV compared to the free chain due to strong mixing with  $z$ -polarized underlying atom vibrations while antisymmetric mode energy decreases and splits due to coupling mainly to laterally polarized vibrations of the NN atoms of the first substrate layer.

Fitting of the sharp high-frequency peaks  $c$ - $f$  gives 1.21, 1.11, 1.31, and 2.43 ps, respectively. Contrary, the lifetime of the in-plane polarized  $b$  mode is 0.35 ps.

### IV. CONCLUSION

We have studied the equilibrium crystal structure and vibrational properties of a single cobalt adatom and simple Co clusters (dimers and trimers) on the low-index Cu surfaces by using interatomic interaction potentials constructed by using the second moment tight-binding approximation.<sup>30,31</sup> We have also done calculations of bond length, binding energy, and vibrations of the free standing clusters  $\text{Co}_2$  and  $\text{Co}_3$ .

It has been shown that in the case of a single Co adatom on all the Cu surfaces of interest, the lowest and the higher frequency modes are determined by the in-plane motion of the adatom and by mixed motion of the nearest-neighbor Cu surface atoms. The highest frequency mode of Co on Cu(111) and Cu(001) is formed by the  $z$ -polarized vibration of the adatom and mixed motion of the Cu NN surface atoms. In contrast, for Co on Cu(110) such mode is characterized by the  $z$ -polarized vibrations of the adatom and nearest-neighbor Cu second layer atom which is located just beneath the Co adatom.

The calculated  $\text{Co}_2$  bond length, binding energy, and the stretch mode frequency are in close agreement with available

experimental data. The interaction of the Co dimer with the substrate leads to vibrations which correspond to translational and rotational degrees of freedom of the free dimer. The low-frequency mode corresponds to the frustrated translation vibration of the dimer along the surface plane. The frustrated rotation mode of the Co dimer on Cu(111) and Cu(001) at 32–34 meV is polarized perpendicular to the surface. For the dimer on Cu(110) the mode at 31.4 meV is the in-plane frustrated rotation vibration of the dimer mixed with vibrations of the NN-1Co and NN-2Co surface atoms.

For all the low-index surfaces, the highest frequency stretch mode of the dimer is split in two, ones due to different interaction of the dimer atoms with the NN-1Co and NN-2Co substrate atoms. On Cu(111) and Cu(100) this splitting is of 4–5 meV. The lower frequency vibration is determined by the interaction with the NN-1Co atoms while the higher frequency vibration is originated from the interaction of the dimer atoms with the NN-2Co substrate atoms. On Cu(110) such splitting of the stretch mode is smaller ( $\approx 2$  meV) due to stronger interaction of the Co atoms with the Cu NN second layer atoms than with Cu surface atoms.

We have demonstrated that the computed frequencies of the isosceles triangle of Co<sub>3</sub> are close to those of the equilateral triangle cluster with one important difference. The lower frequency degenerate mode in the case equilateral triangle splits in two modes because of reduction in symmetry from  $C_{3v}$  to  $C_{2v}$ . It has been shown that the Co equilateral triangle trimer is stable on the Cu(111) surface. On Cu(001) the equilibrium triangle cluster is distorted (isosceles) due to distinct symmetry of the trimer and the substrate surface. On the Cu(110) surface the chain of the three Co adatoms is 0.83 eV lower in energy than the triangle cluster while the free chain is 0.90 eV higher.

As in the case of the dimer, the low-frequency modes of the Co trimer on Cu(111) are the frustrated translation and

frustrated rotation in-plane polarized modes of the cluster. Deformational, antisymmetrical, and symmetrical high-frequency modes of the trimer on Cu(111) are inherited from the free trimer, however, they are split because of different interaction of Co atoms with NN-1Co and NN-2Co Cu atoms by  $\approx 2.5$  meV. On the Cu(001) surface, the Co trimer has the reduced symmetry that leads to polarization of Co vibrations slightly different from those of the Co trimer on Cu(111).

The three Co atoms chain on Cu(110) has the in-plane polarized low-frequency vibrations which correspond to translational and rotational degrees of freedom. In contrast to the unsupported chain where deformational vibrations are of low frequency, on Cu(110) they are of high frequency (31.4 and 34.4 meV for deformational vibrations with in-plane and perpendicular polarization, respectively). Similar to the dimer on Cu(110), the antisymmetrical high-frequency vibration is split by  $\approx 2.5$  meV due to different interaction of the Co trimer atoms with the NN-1Co and NN-2Co substrate atoms. The highest frequency mode is formed by the Co antisymmetrical vibration coupled to the Cu second layer NN atoms and the Cu surface layer NN-2Co atoms.

The longest lifetimes have been found for high-frequency vibrations of all the Co clusters on the low-index Cu surfaces: these lifetimes are of 1–2.5 ps. The shortest lifetimes, 0.1–0.8 ps, have been found for low-frequency horizontal vibrations of the Co clusters.

#### ACKNOWLEDGMENTS

This work was partially supported by the University of the Basque Country (Grant No. 9/UPV 00206.215-13639/2001) and the Spanish Ministerio de Ciencia y Tecnología (Grant No. FIS 2004-06490-C03-01).

\*waptctce@sq.ehu.es

- <sup>1</sup>H. Ibach and D. Bruchmann, *Phys. Rev. Lett.* **44**, 36 (1980).
- <sup>2</sup>R. B. Doak, U. Harten, and J. P. Toennies, *Phys. Rev. Lett.* **51**, 578 (1983).
- <sup>3</sup>G. Benedek, J. Ellis, A. Reichmuth, P. Ruggerone, H. Schief, and J. P. Toennies, *Phys. Rev. Lett.* **69**, 2951 (1992).
- <sup>4</sup>Y. Chen, S. Y. Tong, K. P. Bohnen, T. Rodach, and K. M. Ho, *Phys. Rev. Lett.* **70**, 603 (1993).
- <sup>5</sup>S. E. Finberg, J. V. Lakin, and R. D. Diehl, *Surf. Sci.* **496**, 10 (2002).
- <sup>6</sup>S. Durukanoglu, A. Kara, and T. S. Rahman, *Phys. Rev. B* **55**, 13894 (1997).
- <sup>7</sup>I. Yu. Sklyadneva, G. G. Rusina, and E. V. Chulkov, *Surf. Sci.* **416**, 17 (1998).
- <sup>8</sup>R. Heid and K.-P. Bohnen, *Phys. Rep.* **387**, 151 (2003).
- <sup>9</sup>S. D. Borisova, G. G. Rusina, S. V. Ereemeev, G. Benedek, P. M. Echenique, I. Yu. Sklyadneva, and E. V. Chulkov, *Phys. Rev. B* **74**, 165412 (2006).
- <sup>10</sup>G. G. Rusina, S. V. Ereemeev, P. M. Echenique, G. Benedek, S. D. Borisova, and E. V. Chulkov, *J. Phys.: Condens. Matter* **20**, 224007 (2008).

- <sup>11</sup>G. Benedek and J. P. Toennies, *Surf. Sci.* **299/300**, 587 (1994).
- <sup>12</sup>H. Ibach, *Surf. Sci.* **299/300**, 116 (1994).
- <sup>13</sup>H. Gawronski, M. Mehlhorn, and K. Morgenstern, *Science* **319**, 930 (2008).
- <sup>14</sup>I. Yu. Sklyadneva, E. V. Chulkov, and A. V. Bertsch, *Surf. Sci.* **352-354**, 25 (1996).
- <sup>15</sup>I. Yu. Sklyadneva, G. G. Rusina, and E. V. Chulkov, *Phys. Rev. B* **65**, 235419 (2002).
- <sup>16</sup>J. B. Hannon, E. J. Mele, and E. W. Plummer, *Phys. Rev. B* **53**, 2090 (1996).
- <sup>17</sup>Ph. Hofmann and W. E. Plummer, *Surf. Sci.* **377-379**, 330 (1997).
- <sup>18</sup>M. Lazzeri and S. de Gironcoli, *Surf. Sci.* **402-404**, 715 (1998); **454-456**, 442 (2000).
- <sup>19</sup>Ismail, P. Hofmann, E. W. Plummer, C. Bungaro, and W. Kress, *Phys. Rev. B* **62**, 17012 (2000).
- <sup>20</sup>E. V. Chulkov and I. Yu. Sklyadneva, *Surf. Sci.* **331-333**, 1414 (1995); **345**, 235 (1996) (erratum).
- <sup>21</sup>V. Chis, B. Hellising, G. Benedek, M. Berlusconi, and J. P. Toennies, *J. Phys.: Condens. Matter* **19**, 305011 (2007).
- <sup>22</sup>G. Witte, J. Braun, A. Lock, and J. P. Toennies, *Phys. Rev. B* **52**,

- 2165 (1995).
- <sup>23</sup>M.-C. Marinica, G. Raseev, and K. S. Smirnov, *Phys. Rev. B* **63**, 205422 (2001).
- <sup>24</sup>G. Witte and J. P. Toennies, *Phys. Rev. B* **62**, R7771 (2000).
- <sup>25</sup>P. Rudolf, C. Astaldi, G. Gautero, and S. Modesti, *Surf. Sci.* **251/252**, 127 (1991).
- <sup>26</sup>S.-Å. Lindgren, C. Svensson, L. Walldén, A. Carlsson, and E. Wahlstrom, *Phys. Rev. B* **54**, 10912 (1996).
- <sup>27</sup>G. G. Rusina, S. V. Eremeev, S. D. Borisova, I. Yu. Sklyadneva, and E. V. Chulkov, *Surf. Sci.* **600**, 3921 (2006).
- <sup>28</sup>B. N. J. Persson, *Sliding Friction*, 2nd ed. (Springer, New York, 2000), and references therein.
- <sup>29</sup>B. C. Stipe, M. A. Rezaei, and W. Ho, *Science* **280**, 1732 (1998).
- <sup>30</sup>N. A. Levanov, V. S. Stepanyuk, W. Hergert, D. I. Bazhanov, P. H. Dederichs, A. A. Katsnelson, and C. Massobrio, *Phys. Rev. B* **61**, 2230 (2000).
- <sup>31</sup>V. S. Stepanyuk, D. V. Tsviline, D. I. Bazhanov, W. Hergert, and A. A. Katsnelson, *Phys. Rev. B* **63**, 235406 (2001).
- <sup>32</sup>M. T. Kief and W. F. Egelhoff, *Phys. Rev. B* **47**, 10785 (1993).
- <sup>33</sup>R. Pentcheva and M. Scheffler, *Phys. Rev. B* **61**, 2211 (2000).
- <sup>34</sup>S. Kim, J. Kim, J. Han, J. Seo, C. Lee, and S. Hong, *Surf. Sci.* **453**, 47 (2000).
- <sup>35</sup>F. Nouvertné, U. May, M. Bamming, A. Rampe, U. Korte, G. Güntherodt, R. Pentcheva, and M. Scheffler, *Phys. Rev. B* **60**, 14382 (1999).
- <sup>36</sup>D. V. Tsvilin, V. S. Stepanyuk, W. Hergert, and J. Kirshner, *Phys. Rev. B* **68**, 205411 (2003).
- <sup>37</sup>R. A. Miron and K. A. Fichthorn, *Phys. Rev. Lett.* **93**, 128301 (2004).
- <sup>38</sup>R. A. Miron and K. A. Fichthorn, *Phys. Rev. B* **72**, 035415 (2005).
- <sup>39</sup>J. A. Stroschio and R. J. Celotta, *Science* **306**, 242 (2004).
- <sup>40</sup>Kai Liu and Shiwu Gao, *Phys. Rev. Lett.* **95**, 226102 (2005).
- <sup>41</sup>Kai Liu and Shiwu Gao, *Phys. Rev. B* **74**, 195433 (2006).
- <sup>42</sup>V. Rosato, B. Guillope, and B. Legrand, *Philos. Mag. A* **59**, 321 (1989); F. Cleri and V. Rosato, *Phys. Rev. B* **48**, 22 (1993).
- <sup>43</sup>K. Wildberger, V. S. Stepanyuk, P. Lang, R. Zeller, and P. H. Dederichs, *Phys. Rev. Lett.* **75**, 509 (1995).
- <sup>44</sup>K. Sastry, D. D. Johnson, D. E. Goldberg, and P. Bellon, *Phys. Rev. B* **72**, 085438 (2005).
- <sup>45</sup>V. S. Stepanyuk, A. L. Klavsyuk, L. Niebergall, A. M. Saletsky, W. Hergert, and P. Bruno, *Phase Transitions* **78**, 61 (2005).
- <sup>46</sup>R. A. Miron and K. A. Fichthorn, *Phys. Rev. B* **72**, 035415 (2005).
- <sup>47</sup>N. N. Negulyaev, V. S. Stepanyuk, W. Hergert, P. Bruno, and J. Kirshner, *Phys. Rev. B* **77**, 085430 (2008).
- <sup>48</sup>O. Mironets, H. L. Meyerheim, C. Tusche, V. S. Stepanyuk, E. Soyka, P. Zschack, H. Hong, N. Jeutter, R. Felici, and J. Kirshner, *Phys. Rev. Lett.* **100**, 096103 (2008).
- <sup>49</sup>A. Kant and B. Strauss, *J. Chem. Phys.* **41**, 3806 (1964).
- <sup>50</sup>S. Datta, M. Kabir, S. Ganguly, B. Sanyal, T. Saha-Dasgupta, and A. Mookerjee, *Phys. Rev. B* **76**, 014429 (2007).
- <sup>51</sup>M. Castro, C. Jamorski, and D. R. Salahub, *Chem. Phys. Lett.* **271**, 133 (1997).
- <sup>52</sup>A. N. Andriotis and M. Menon, *Phys. Rev. B* **57**, 10069 (1998).
- <sup>53</sup>D. A. Hales, C. X. Su, L. Lian, and P. B. Armentrout, *J. Chem. Phys.* **100**, 1049 (1994).
- <sup>54</sup>K. H. Chae, H. C. Lu, and T. Gustafsson, *Phys. Rev. B* **54**, 14082 (1996).
- <sup>55</sup>K. P. Bohnen and K. M. Ho, *Surf. Sci. Rep.* **19**, 99 (1993).
- <sup>56</sup>L. Yang, T. S. Rahman, and M. S. Daw, *Phys. Rev. B* **44**, 13725 (1991).
- <sup>57</sup>J. S. Nelson, E. C. Sowa, and M. S. Daw, *Phys. Rev. Lett.* **61**, 1977 (1988).
- <sup>58</sup>H. L. Davis and J. R. Noonan, *J. Vac. Sci. Technol.* **20**, 842 (1982).
- <sup>59</sup>Q. T. Jiang, P. Fenter, and T. Gustafsson, *Phys. Rev. B* **44**, 5773 (1991).
- <sup>60</sup>D. L. Adams, H. B. Nielsen, J. N. Andersen, I. Stensgaard, R. Feidenhans'l, and J. E. Sørensen, *Phys. Rev. Lett.* **49**, 669 (1982).
- <sup>61</sup>H. L. Davis and J. R. Noonan, *Surf. Sci.* **126**, 245 (1983).
- <sup>62</sup>M. H. Mohamed, L. L. Kesmodel, Burl M. Hall and D. L. Mills, *Phys. Rev. B* **37**, 2763 (1988).
- <sup>63</sup>U. Harten, J. P. Toennies, and Ch. Wöll, *Faraday Discuss. Chem. Soc.* **80**, 137 (1985).
- <sup>64</sup>M. Wuttig, R. Franchy, and H. Ibach, *Z. Phys. B: Condens. Matter* **65**, 71 (1986).
- <sup>65</sup>P. Zeppenfeld, K. Kern, R. David, K. Kuhnke, and G. Comsa, *Phys. Rev. B* **38**, 12329 (1988).
- <sup>66</sup>D. G. Leopold and W. C. Lineberger, *J. Chem. Phys.* **85**, 51 (1986).
- <sup>67</sup>D. P. DiLella, W. Limm, R. H. Lipson, M. Moskovits, and K. V. Taylor, *J. Chem. Phys.* **77**, 5263 (1982).